A parsimonious analytical model for simulating two-dimensional multispecies plume migration

Jui-Sheng Chen[a], Ching-Ping Liang[b], Chen-Wuing Liu[c,]*, Loretta Y. Li [d]

[a]*Graduate Institute of Applied Geology, National Central University, Jhongli, Taoyuan 32001, Taiwan*

[b]*Department of Environmental Engineering and Science,Fooyin University, Kaohsiung 83101, Taiwan*

[c]*Department of Bioenvironmental Systems Engineering, National Taiwan University, Taipei 10617, Taiwan*

[d]*Department of Civil Engineering, University of British Columbia, Vancouver, BC V6T 1Z4, Canada*

**Corresponding author: Chen-Wuing Liu, Department of Bioenvironmental Systems Engineering, National Taiwan University, Taipei 10617, Taiwan*

E-mail: cwliu@ntu.edu.tw

Tel: +886-2-23626480

Abstract

The two-dimensional advection-dispersion equations coupled with sequential first-order decay reactions involving arbitrary number of species in groundwater system is considered to predict the two-dimensional plume behavior of decaying contaminant such as radionuclide and dissolved chlorinated solvent. Generalized analytical solutions in compact format are derived through the sequential application of the Laplace, finite Fourier cosine, and generalized integral transform to reduce the coupled partial differential equation system to a set of linear algebraic equations. The system of algebraic equations is next solved for each species in the transformed domain, and the solutions in the original domain are then obtained through consecutive integral transform inversions. Explicit form solutions for a special case are derived using the generalized analytical solutions and are compared with the numerical solutions. The analytical results indicate that the analytical solutions are robust, accurate and useful for simulation or screening tools to assess plume behaviors of decaying contaminants.

Keywords: Parsimonious analytical model; reactive transport; first-order decay reaction; Bateman-type source; radionuclide; dissolved chlorinated solvent.

1. Introduction

Experimental and theoretical studies have been undertaken to understand the fate and transport of dissolved hazardous substances in subsurface environments because that human health is threatened by a wide spectrum of contaminants in groundwater and soil. Analytical models are essential and efficient tools for understanding pollutants behavior in subsurface environments. Several analytical solutions for single-species transport problems have been reported for simulating the transport of various contaminants (Batu, 1989; 1993; 1996; Chen et al., 2008a; 2008b; 2011; Gao et al., 2010; 2012; 2013; Leij et al., 1991; 1993; Park and Zhan, 2001; Pérez Guerrero and Skaggs, 2010 ; Pérez Guerrero et al., 2013 ; van Genuchten and Alves, 1982; Yeh, 1981; Zhan et al., 2009; Ziskind et al., 2011). Transport processes of some contaminants such as radionuclides, dissolved chlorinated solvents and nitrogen generally involve a series of first-order or pseudo first-order sequential decay chain reactions. During migrations of decaying contaminants, mobile and toxic successor products may sequentially form and move downstream with elevated concentrations. Single-species analytical models do not permit transport behaviors of successor species of these decaying contaminants to be evaluated. Analytical models for multispecies transport equations coupled with first-order sequential decay reactions are useful tools for synchronous determination of the fate and transport of the predecessor and successor species of decaying contaminants. However, there are few analytical solutions for coupled multispecies transport equations compared to a large body of analytical solutions in the literature pertaining to the single-species advective-dispersive transport subject to a wide spectrum of initial and boundary conditions.

Mathematical approaches have been proposed in the literature to derive a limited number of one-dimensional analytical solutions or semi-analytical solutions for multispecies advective–dispersive transport equations sequentially coupled with first-order decay reactions. These include direct integral transforms with sequential substitutions (Cho, 1971; Lunn et al., 1996; van Genuchten, 1985, Mieles

and Zhan, 2012), decomposition by change-of-variables with the help of existing single-species analytical solutions (Sun and Clement, 1999; Sun et al., 1999a; 1999b), Laplace transform combined with decomposition of matrix diagonization (Quezada et al., 2004; Srinivasan and Clememt, 2008a; 2008b), decomposition by change-of-variables coupled with generalized integral transform (Pérez Guerrero et al., 2009; 2010), sequential integral transforms in association with algebraic decomposition (Chen et al., 2012a; 2012b).

Multi-dimensional solutions are needed for real world applications, making them more attractive than one-dimensional solutions. Bauer et al. (2001) presented the first set of semi-analytical solutions for one-, two-, and three-dimensional coupled multispecies transport problem with distinct retardation coefficients. Explicit analytical solutions were derived by Montas (2003) for multi-dimensional advective-dispersive transport coupled with first-order reactions for a three-species transport system with distinct retardation coefficients of species. Quezada et al. (2004) extended the Clement (2001) strategy to obtain Laplace-domain solutions for an arbitrary decay chain length. Most recently, Sudicky et al. (2013) presented a set of semi-analytical solutions to simulate the three-dimensional multi-species transport subject to first-order chain-decay reactions involving up to seven species and four decay levels. Basically, their solutions were obtained species by species using recursion relations between target species and its predecessor species. For a straight decay chain, they derived solutions for up to four species and no generalized expressions with compact formats for any target species were obtained. Note that their solutions were derived for the first-type (Dirichlet) inlet conditions which generally bring about physically improper mass conservation and significant errors in predicting the concentration distributions especially for a transport system with a large longitudinal dispersion coefficient (Barry and Sposito, 1988; Parlange et al., 1992). Moreover, in addition to some special cases, the numerical Laplace transforms are required to obtain the original time domain solution. Besides the straight decay chain, the analytical model by Clement (2001) and Sudicky (2013) can

account for more complicated decay chain problems such as diverging, converging and branched decay chains**.**

Based on the aforementioned reviews, this study presents a parsimonious explicit analytical model for two-dimensional multispecies transport coupled by a series of first-order decay reactions involving an arbitrary number of species in groundwater system. The derived analytical solutions have four salient features. First, the third-type (Robin) inlet boundary conditions which satisfy mass conservation are considered. Second, the solution is explicit, thus solution can be easily evaluated without invoking the numerical Laplace inversion. Third, the generalized solutions with parsimonious mathematical structures are obtained and valid for any species of a decay chain. The parsimonious mathematical structures of the generalized solutions are easy to code into a computer program for implementing the solution computations for arbitrary target species. Fourth, the derived solutions can account for any decay chain length. The explicit analytical solutions have applications for evaluation of concentration distribution of arbitrary target species of the real-world decaying contaminants. The developed parsimonious model is robustly verified with three example problems and applied to simulate the multispecies plume migration of dissolved radionuclides and chlorinated solvent.

2. Governing equations and analytical solutions

2.1 Derivation of analytical solutions

This study consider the problem of decaying contaminant plume migration. The source zone is located in the upstream of groundwater flow. The source zone can represent leaching of radionuclide from a radioactive waste disposal facility or release of chlorinated solvent from the residual NAPL phase into the aqueous phase. After these decaying contaminants enter the aqueous phase, they migrate by one-dimensional advection with flowing groundwater and by simultaneously longitudinal and transverse dispersion processes. While migrating in the groundwater system, the contaminants undergo

linear isothermal equilibrium sorption and a series of sequential first-order decaying reactions. Sudicky et al. (2013) provided the detailed modeling scenario. The scenario considered in this study can be ideally described as shown in Fig. 1. A steady and uniform velocity in the x direction is considered in Fig. 1. The governing equations describing two-dimensional reactive transport of the decaying contaminants and their successor species undergoing linear isothermal equilibrium sorption and a series of sequential first-order decaying reactions can be mathematically written as

$$D_L \frac{\partial^2 C_1(x,y,t)}{\partial x^2} - v\frac{\partial C_1(x,y,t)}{\partial x} + D_T \frac{\partial^2 C_1(x,y,t)}{\partial y^2} - k_1 R_1 C_1(x,y,t) = R_1 \frac{\partial C_1(x,y,t)}{\partial t} \quad (1a)$$

$$D_L \frac{\partial^2 C_i(x,y,t)}{\partial x^2} - v\frac{\partial C_i(x,y,t)}{\partial x} + D_T \frac{\partial^2 C_i(x,y,t)}{\partial y^2} - k_i R_i C_i(x,y,t) + k_{i-1} R_{i-1} C_{i-1}(x,y,t) = R_i \frac{\partial C_i(x,y,t)}{\partial t} \quad i = 2...N. \quad (1b)$$

where $C_i(x,y,t)$ is the aqueous concentration of species i [$\mathbf{ML^{-3}}$]; x and y are the spatial coordinates in the groundwater flow and perpendicular directions [**L**], respectively; t is time [**T**]; D_L and D_T represent the longitudinal and transverse dispersion coefficients [$\mathbf{L^2T^{-1}}$], respectively; v is the average steady and uniform pore-water velocity [$\mathbf{LT^{-1}}$]; k_i is the first-order decay rate constant of species i [$\mathbf{T^{-1}}$]; R_i is the retardation coefficient of species i [-]. Note that these equations consider that the decay reactions occur simultaneously in both the aqueous and sorbed phases. If the decay reactions occur only in the aqueous phase, the retardation coefficients in the decay terms in the right-hand sides of Eqs. (1a) and (1b) become unity. For such case, k_i and k_{i-1} in the left-hand sides could be modified as $\frac{k_i}{R_i}$ and $\frac{k_{i-1}}{R_{i-1}}$ to facilitate the application of the derived analytical solutions obtained by Eqs. (1a) and (1b).

130 The initial and boundary conditions for solving Eqs. (1a) and (1b) are:

131 $$C_i(x,y,t=0)=0 \quad 0\le x\le L, 0\le y\le W \qquad i=1...N. \tag{2}$$

132 $$-D_L\frac{\partial C_i(x=0,y,t)}{\partial x}+vC_i(x=0,y,t)=vf_i(t)\left[H(y-y_1)-H(y-y_2)\right] \qquad t\ge 0 \qquad i=1...N. \tag{3}$$

133 $$\frac{\partial C_i(x=L,y,t)}{\partial x}=0 \qquad t\ge 0, 0\le y\le W \qquad i=1...N. \tag{4}$$

134 $$\frac{\partial C_i(x,y=0,t)}{\partial y}=0 \qquad t\ge 0, 0\le x\le L \qquad i=1...N. \tag{5}$$

135 $$\frac{\partial C_i(x,y=W,t)}{\partial y}=0 \qquad t\ge 0, 0\le x\le L \qquad i=1...N. \tag{6}$$

136 where $f_i(t)$ is the arbitrary time-dependent source concentration of species *i* applied at the source
137 segment ($H(y-y_1)-H(y-y_2)$) at boundary (x = 0) which will be specified later [L], $H(\bullet)$ is the
138 Heaviside function, L and W are the length and width of the transport system under consideration
139 [L]. Eq. (2) implies that the transport system is free of solute mass at the initial time.
140 Eq. (3) means that a third-type boundary condition satisfying mass conservation at the inlet boundary
141 is considered. Eq. (4) considers the concentration gradient to be zero at the exit boundary based on
142 the mass conservation principle. Such a boundary condition has been widely used for simulating
143 solute transport in a finite-length system. Eqs. (5) and (6) assume no solute flux across the lower and
144 upper boundaries. It is noted that in Eq. (3), we assume arbitrary time-dependent sources of species *i*
145 uniformly distributed at the segment ($y_1\le y\le y_2$) of the inlet boundary ($x=0$), the so-called
146 Heaviside function source concentration profile. Relative to the first type boundary conditions used
147 by Sudicky et al. (2013), the third-type boundary conditions which satisfy mass conservation at the
148 inlet boundary (Barry and Sposito, 1988; Parlange et al., 1992) are used herein. Sudicky et al. (2013)
149 considered the source concentration profiles as Gaussian or Heaviside step functions. If Gaussain
150 distributions are desired, we can easily replace the Heaviside function in the right-hand side of Eq.

(3) with a Gaussian distribution.

Eqs. (1)-(6) can be expressed in dimensionless form as

$$\frac{1}{Pe_L}\frac{\partial^2 C_1(X,Y,Z)}{\partial X^2}-\frac{\partial C_1(X,Y,Z)}{\partial X}+\frac{\rho^2}{Pe_T}\frac{\partial^2 C_1(X,Y,Z)}{\partial Y^2}-\kappa C_1(X,Y,Z)=R_1\frac{\partial C_1(X,Y,T)}{\partial T} \tag{7a}$$

$$\begin{aligned}&\frac{1}{Pe_L}\frac{\partial^2 C_i(X,Y,T)}{\partial X^2}-\frac{\partial C_i(X,Y,T)}{\partial X}+\frac{\rho^2}{Pe_T}\frac{\partial^2 C_i(X,Y,T)}{\partial Y^2} \quad i=2...N. \\ &-\kappa_i C_i(X,Y,T)+\kappa_{i-1}C_{i-1}(X,Y,T)=R_i\frac{\partial C_i(X,Y,T)}{\partial T}\end{aligned} \tag{7b}$$

$$C_i(X,Y,T=0)=0 \quad 0\le X\le 1, 0\le Y\le 1 \quad i=1...N. \tag{8}$$

$$-\frac{1}{Pe_L}\frac{\partial C_i(X=0,Y,T)}{\partial X}+C_i(X=0,Y,Z)=f_i(T)\left[H(Y-Y_1)-H(Y-Y_2)\right]\ T\ge 0, i=1...N. \tag{9}$$

$$\frac{\partial C_i(X=1,Y,T)}{\partial X}=0 \quad T\ge 0, 0\le Y\le 1 \quad i=1...N. \tag{10}$$

$$\frac{\partial C_i(X,Y=0,T)}{\partial Y}=0 \quad T\ge 0, 0\le X\le 1 \quad i=1...N. \tag{11}$$

$$\frac{\partial C_i(X,Y=1,T)}{\partial Y}=0 \quad T\ge 0, 0\le X\le 1 \quad i=1...N. \tag{12}$$

where $X=\frac{x}{L}$, $Y=\frac{y}{W}$, $Y_1=\frac{y_1}{W}$, $Y_2=\frac{y_2}{W}$, $T=\frac{vt}{L}$, $Pe_L=\frac{vL}{D_L}$, $Pe_T=\frac{vL}{D_T}$, $\rho=\frac{L}{W}$.

Our solution strategy used is extended from the approach proposed by Chen at al. (2012a; 2012b). The core of this approach is that the coupled partial differential equations are converted into an algebraic equation system via a series of integral transforms and the solutions in the transformed domain for each species are directly and algebraically obtained by sequential substitutions.

Following Chen et al. (2012a; 2012b), the generalized analytical solutions in compact formats can be obtained as follows (with detailed derivation provided in Appendix A)

$$C_i(X,Y,T)$$

$$= f_i(T)\Phi(n=0) + e^{\frac{Pe_L}{2}X}\sum_{l=1}^{\infty}\frac{K(\xi_l,X)}{N(\xi_l)}\left[p_i(\xi_l,n,T)+q_i(\xi_l,n,T)\right]\Phi(n=0)\Theta(\xi_l) \quad (13)$$

$$+2\sum_{n=1}^{n=\infty}\left\{f_i(T)\Phi(n)+e^{\frac{Pe_L}{2}X}\sum_{l=1}^{\infty}\frac{K(\xi_l,X)}{N(\xi_l)}\left[p_i(\xi_l,n,T)+q_i(\xi_l,n,T)\right]\Phi(n)\Theta(\xi_l)\right\}\cos(n\pi Y)$$

where $\Phi(n)=\begin{cases}Y_2-Y_1 & n=0\\ \dfrac{\sin(n\pi Y_2)-\sin(n\pi Y_1)}{n\pi} & n=1,2,3...\end{cases}$, ξ_l is the eigenvalue, determined from the equation $\xi_l\cot\xi_l-\dfrac{{\xi_l}^2}{Pe_L}+\dfrac{Pe_L}{4}=0$, $\Theta(\xi_l)=\dfrac{Pe_L\xi_l}{\frac{{Pe_L}^2}{4}+{\xi_l}^2}$, $K(\xi_l,X)=\dfrac{Pe_L}{2}\sin(\xi_l X)+\xi_l\cos(\xi_l X)$,

$$N(\xi_l)=\frac{2}{\frac{{Pe_L}^2}{4}+Pe_L+{\xi_l}^2},$$

$$p_i(\xi_l,n,T)=f_i(T)-\beta_i e^{-\alpha_i T}\int_0^T f_i(\tau)e^{\alpha_i\tau}d\tau \quad (14)$$

and

$$q_i(\xi_l,n,T)=\sum_{k=0}^{k=i-2}\left(\beta_{i-k-1}\prod_{j_1=0}^{j_1=k}\sigma_{i-j_1}\right)\sum_{j_2=0}^{j_2=k+1}\frac{e^{-\alpha_{i-j_2}T}\int_0^T e^{\alpha_{i-j_2}\tau}f_{i-k-1}(\tau)d\tau}{\prod_{j_3=i-k-1,\,j_3\neq i-j_2}^{j_3=i}\left(\alpha_{j_3}-\alpha_{i-j_2}\right)} \quad (15)$$

where $\alpha_i(\xi_l)=\dfrac{\kappa_i}{R_i}+\dfrac{\rho^2n^2\pi^2}{Pe_T R_i}+\dfrac{Pe_L}{4R_i}+\dfrac{{\xi_l}^2}{Pe_L R_i}$, $\beta_i(\xi_l)=\dfrac{Pe_L}{4R_i}+\dfrac{{\xi_l}^2}{Pe_L R_i}$, $\sigma_i=\dfrac{\kappa_{i-1}}{R_i}$

Concise expressions for arbitrary target species such as described in Eqs. (13) to (15) facilitate the development of a computer code for implementing the computations of the analytical solutions.

The generalized solutions of Eq. (13) accompanied by two corresponding auxiliary functions $p_i(\xi_l,n,T)$ and $q_i(\xi_l,n,T)$ in Eqs. (14)-(15) can be applied to derive analytical solutions for some

special-case inlet boundary sources. Here the time-dependent decaying source which represents the specific release mechanism defined by the Bateman equations (van Genuchten, 1985) is considered. A Bateman-type source is described by

$$f_i(t) = \sum_{m=1}^{i} b_{im} e^{-\delta_m t} \tag{16a}$$

or in dimensionless form,

$$f_i(T) = \sum_{m=1}^{m=i} b_{in} e^{-\lambda_m T} \tag{16b}$$

The coefficients b_{im} and $\delta_m = \mu_m + \gamma_m$ account for the first-order decay reaction rate (μ_m) of each species in the waste source and the release rate (γ_m) of each species from the waste source, $\lambda_m = \frac{\delta_m L}{v}$.

By substituting Eq. (16b) into Eqs. (13)-(15), we obtain

$$\begin{aligned} & C_i(X,Y,T) \\ & = \sum_{m=1}^{m=i} b_{im} e^{-\lambda_m T} \Phi(n=0) + e^{\frac{Pe_L}{2} X} \sum_{l=1}^{\infty} \frac{K(\xi_l, X)}{N(\xi_l)} \left[p_i(\xi_l, n, T) + q_i(\xi_l, n, T) \right] \Phi(n=0) \Theta(\xi_l) \\ & + 2 \sum_{n=1}^{n=\infty} \left\{ \sum_{m=1}^{m=i} b_{im} e^{-\lambda_m T} \Phi(n) + e^{\frac{Pe_L}{2} X} \sum_{l=1}^{\infty} \frac{K(\xi_l, X)}{N(\xi_l)} \left[p_i(\xi_l, n, T) + q_i(\xi_l, n, T) \right] \Phi(n) \Theta(\xi_l) \right\} \cos(n\pi Y) \end{aligned} \tag{17}$$

where

$$p_i(\xi_l, n, T) = \sum_{m=1}^{m=i} b_{i,m} \cdot e^{-\lambda_m T} - \beta_i \sum_{m=1}^{m=i} b_{i,m} \frac{e^{-\lambda_m T} - e^{-\alpha_i T}}{\alpha_i - \lambda_m} \tag{18}$$

and

$$p_i(\xi_l,n,T)=\sum_{k=0}^{k=i-2}\left(\beta_{i-k-1}\prod_{j_1=0}^{j_1=k}\sigma_{i-j_1}\right)\sum_{j_2=0}^{j_2=k+1}\frac{\sum_{m=1}^{m=i-k-1}\frac{b_{i-k-1,m}\left(e^{-\lambda_m T}-e^{-\alpha_{i-j_2}T}\right)}{\alpha_{i-j_2}-\lambda_m}}{\prod_{j_3=i-k-1,\,j_3\neq i-j_1}^{j_3=i}\left(\alpha_{j_3}-\alpha_{i-j_2}\right)} \tag{19}$$

Based on the special-case analytical solutions in Eq. (17) supported by two auxiliary functions, defined in Eqs. (18) and (19), a computer code was developed in FORTRAN 90 language with double precision. The details of the FORTRAN computer code are described in Supplement. Using the required numbers determined from the convergence test, the computational time for evaluation of the solutions at 50 different observations only takes 3.782s, 11.325s, 23.95s and 67.23s computer clock time on an Intel Core i7-2600 3.40 MHz PC for species 1, 2, 3, and 4 in the comparison of example 1.

3. Results and discussion

3.1 Convergence behavior of the Bateman-type source solution

The derived analytical solutions in Eqs. (17)-(19) consist of summations of double infinite series expansions for the finite Fourier cosine and generalized integral transform inversions, respectively. It is straightforward to sum up these two infinite series expansions term by term. To avoid time-consuming summations of these infinite series expansions, the convergence tests should be routinely executed to determine the optimal number of the required terms for evaluating analytical solutions to the desired accuracies. Two-dimensional four-member radionuclide decay chain $^{238}Pu \rightarrow ^{234}U \rightarrow ^{230}Th \rightarrow ^{226}Ra$ is considered herein as convergence test example 1 to demonstrate the convergence behavior of the series expansions. This convergence test example 1 is modified from a one-dimensional radionuclide decay chain problem originated by Higashi and Pigford (1980) and later applied by van Genuchten (1985) to illustrate the applicability of their derived solution. The

215 important model parameters related to this test example are listed in Tables 1 and 2. The inlet source
216 is chosen to be symmetrical with respect to the x-axis and conveniently arranged in the
217 $40\,m \le y \le 60\,m$ segment at the inlet boundary.

218 In order to determine the optimal term number of series expansions for the finite Fourier cosine
219 transform inverse to achieve accurate numerical evaluation, we specify a sufficiently large number of
220 series expansions for the generalized transform inverse so that the influence of the number of series
221 expansions can be precluded. A similar concept is used when investigating the required number of
222 terms in the series expansions for the generalized integral transform inverse. An alternative approach
223 is conducted by simultaneously varying the term numbers of series expansions for the generalized
224 integral transform inverse and the finite Fourier cosine transform inverse.

225 Tables 3, 4 and 5 give results of the convergence tests up to 3 decimal digits of the solution
226 computations along the three transects (inlet boundary at x=0 m, x=25 m, and exit boundary at x
227 =250m). In these tables M and N are defined as the numbers of terms summed for the generalized
228 integral transform inverse and finite Fourier cosine transform inverse, respectively. It is observed that
229 M and N are related closely to the true values of the solutions. For smaller true values, the solutions
230 must be computed with greater M and N. However, convergences can be drastically speeded up if
231 lower calculation precision (e.g. 2 decimal digits accuracy) is acceptable. For example,
232 $(M, N) = (100,200)$ is sufficient for 2 decimal digits accuracy, while for 3 decimal digits accuracy we
233 need $(M, N) = (1600,8000)$. Two decimal digits accuracy is acceptable for most practical problems. It
234 is also found that M increases and N decreases with increasing x.

235 To further examine the series convergence behavior, example 2 considers a transport system of
236 large aspect ratio ($\frac{L}{W} = \frac{2{,}500m}{100m}$) and a narrower source segment, $45\,m \le y \le 55\,\text{m}$, on the inlet
237 boundary. Tables 6 and 7 present results of the convergence tests of the solution computations along

two transects (inlet boundary and x =250 m). Tables 6 and 7 also show similar results for the dependences of M and N on x. Note that larger M and N are required for each species in this test example, suggesting that the evaluation of the solution for a large aspect ratio requires more series expansion terms to achieve the same accuracy as compared to example 1. Detailed results of the convergence test examples 1 and 2 are provided in Supplement.

3.2 Comparison of the analytical solutions with the numerical solutions

Three comparison examples are considered to examine the correctness and robustness of the analytical solutions and the accuracy of the computer code. The first comparison example is the four-member radionuclide transport problem used in the convergence test example 1. The second comparison example considers the four-member radionuclide transport problem used in the convergence test example 2. The third comparison example is used to test the accuracy of the computer code for simulating the reactive contaminant transport of a long decay chain. The three comparison examples are executed by comparing the simulated results of the derived analytical solutions with the numerical solutions obtained using the Laplace transformed finite difference (LTFD) technique first developed by Moridis and Reddell (1991). A computer code for the LTFD solution are written in FORTTRAN language with double precision. The details of the FORTRAN computer code is described in Supplement.

Figures 2, 3 and 4 depicts the spatial concentration distribution along one longitudinal direction ($y = 50$ m) and two transverse directions ($x = 0$ m and $x = 25$ m) for convergence test example 1 at t = 1,000 year obtained from analytical solutions and numerical solutions. Figures 5, 6 and 7 present the spatial concentration distribution along one longitudinal direction ($y = 50$ m) and two transverse directions ($x = 0$ m and $x = 25$ m) for the convergence test example 2 at t = 1,000 year obtained from analytical solutions and numerical solutions. Excellent agreements between the two solutions for

both examples are observed for a wide spectrum of concentration, thus warranting the accuracy and robustness of the developed analytical model.

The third example involves a 10 species decay chain previously presented by Srinivasan and Clement (2008a) to evaluate the performance of their one-dimensional analytical solutions. The relevant model parameters are summarized in Tables 8 and 9. Our computer code is also compared against the LTFD solutions for this example. Figure 8 depicts the spatial concentration distribution at t = 20 days obtained analytically and numerically. Again there is excellent agreement between the analytical and numerical solutions, demonstrating the performance of our computer code for simulating transport problems with a long decay chain. The three comparison results clearly establish the correctness of the analytical model and the accuracy and capability of the computer code.

3.3 Assessing physical and chemical parameters on the radionuclide plume migration

Physical processes and chemical reactions affect the extent of contaminant plumes, as well as concentration levels. To illustrate how the physical processes and chemical reactions affect multispecies plume development, we consider the four-member radionuclide decay chain used in the previous convergence test and solution verification. The model parameters are the same, except that the longitudinal (D_L) and transverse (D_T) dispersion coefficients are varied. Three sets of longitudinal and transverse dispersion coefficients D_L =1,000, D_T =100; D_L =1,000, D_T =200; D_L =2000, D_T =200 (all in m^2/year) are tested, all for a simulation time of 1,000 years.

Figure 9 illustrates the spatial concentration of four species at t = 1,000 year for the three sets of dispersion coefficients. The mobility of plumes of ^{234}U and ^{230}Th is retarded because of their stronger sorption ability. Hence the least retarded ^{226}Ra plume extensively migrated to 200 m × 60 m area in the simulation domain, whereas the ^{234}U and ^{230}Th plumes are confined within 60 m × 50 m area

285 in the simulation domain. The moderate mobility of ^{238}Pu reflects the fact that it is a medial sorbed
286 member of this radionuclide decay chain. The high concentration level of ^{234}U accounts for the high
287 first-order decay rate constant of its parent species ^{238}Pu and its own low first-order decay rate constant.
288 The plume extents and concentration levels may be sensitive to longitudinal and transverse dispersion.
289 Increase of the longitudinal and/or transverse dispersion coefficients enhances the spreading of the
290 plume extensively along the longitudinal and/or transverse directions, thereby lowering the plume
291 concentration level. Because the concentration levels of the four radionuclides are influenced by both
292 source release rates and decay chain reactions, ^{230}Th has the least extended plume area, while ^{226}Ra
293 has the greatest plume area for all three set of dispersion coefficients. These dispersion coefficients
294 only affect the size of plumes of the four radionuclide, but the order of their relative plume size remains
295 the same (i.e. $^{226}Ra > {}^{238}Pu > {}^{234}U > {}^{230}Th$ for the simulated condition). Indeed, in the reactive
296 contaminant transport, the chemical parameters of sorption and decay rate are more important than the
297 physical parameters of dispersion coefficients that govern the order of the plume extents and the
298 concentration levels.
299
300 *3.4 Simulating the natural attenuation of chlorinated solvent plume migration*
301 Natural attenuation is the reduction in concentration and mass of the contaminant due to
302 naturally occurring processes in the subsurface environment. The process is monitored for regulatory
303 purposes to demonstrate continuing attenuation of the contaminant reaching the site-specific
304 regulatory goals within reasonable time, hence, the use of the term monitored natural attenuation
305 (MNA). MNA has been widely accepted as a suitable management option for chlorinated solvent
306 contaminated groundwater. Mathematical model are widely used to evaluate the natural attenuation
307 of plumes at chlorinated solvent sites. The multispecies transport analytical model developed in this
308 study provides an effective tool for evaluating performance of the monitoring natural attenuation of

plumes at a chlorinated solvent site because a series of daughter products produced during biodegradation of chlorinated solvent such as *PCE→TCE→DCE→VC→ETH*. Thus simulation of the natural attenuation of plumes a chlorinated solvent constitutes an attractive field application example of our multispecies transport model.

A study of 45 chlorinated solvent sites by McGuire et al. (2014) found that mathematical models were used at 60% of these sites and that the public domain model BIOCHLOR (Aziz et al., 2000) provided by the Center for Subsurface Modeling Support (CSMoS) of USEPA was the most commonly used model. An illustrated example from BIOCHLOR manual (Aziz et al., 2000) is considered to demonstrate the application of the developed analytical model. This example application demonstrated that BIOCHLOR can reproduce plume movement from 1965 to 1998 at the contaminated site of Cape Canaveral Air Station, Florida. The simulation conditions and transport parameters for this example application are summarized in Table 10. Constant source concentrations rather than exponentially declining source concentration of five-species chlorinated solvents are specified in the $90.7\, m \le y \le 122.7\, m$ segment at the inlet boundary ($x = 0$). This means that the exponents (λ_{im}) of Bateman-type sources in Eqs. (16a) or (16b) need to be set to zero for the constant source concentrations and source intensity constants (b_{im}) are set to zero when subscript *i* does not equal to subscript *m.* Table 11 lists the coefficients of Bateman-type boundary source used for this example application involving the five-species dissolved chlorinated solvent problem. Spatial concentration contours of five-species at t = 1 year obtained from the derived analytical solutions for natural attenuation of chlorinated solvent plumes are depicted in Fig. 10. It is observed that the mobility of plumes is quite sensitive to the species retardation factors, whereas the decay rate constants determine the plume concentration level. The plumes can migrate over a larger region for species having a low retardation factor such as VC. The low decay rate constants such as ETH have higher concentration distribution than the VC. It should be noted that a larger extent of plume

observed for ETH in Fig. 10 is mainly attributed the plume mass accumulation from the predecessor species VC that have a larger plume extent. The effect of high retardation of the ETH is hindered by the mass accumulation of the predecessor species VC.

4. Conclusions

We present an analytical model with a parsimonious mathematical format for two-dimensional multispecies advective-dispersive transport of decaying contaminants such as radionuclides, chlorinated solvents and nitrogen. The developed model is capable of accounting for the temporal and spatial development of an arbitrary number of sequential first-order decay reactions. The solution procedures involve applying a series of Laplace, finite Fourier cosine and generalized integral transforms to reduce a partial differential equation system to an algebraic system, solving for the algebraic system for each species, and then inversely transforming the concentration of each species in transformed domain into the original domain. Explicit special solutions for Bateman type source problems are derived via the generalized analytical solutions. The convergence of the series expansion of the generalized analytical solution is robust and accurate. These explicit solutions and the computer code are comparing with the results computed by the numerical solutions. The two solutions agree well for a wide spectrum of concentration variations for three test examples. The analytical model is applied to assess the plume development of radionuclide and dissolved chlorinated solvent decay chain. The results show that dispersion only moderately modifies the size of the plumes, without altering the relative order of the plume sizes of different contaminant. It is suggested that retardation coefficients, decay rate constants and the predecessor species plume distribution mainly govern the order of plume size in groundwater. Although there are a number of numerical reactive transport models that can account for multispecies advective-dispersive transport, our analytical model with a computer code that can directly evaluate the two-dimensional temporal-spatial concentration distribution of arbitrary

target species without involving the computation of other species. The analytical model developed in this study effectively and accurately predicts the two-dimensional radionuclide and dissolved chlorinated plume migration. It is a useful tool for assessing the ecological and environmental impact of the accidental radionuclide releases such as the Fukushima nuclear disaster where multiple radionuclides leaked through the reactor, subsequently contaminating the local groundwater and ocean seawater in the vicinity of the nuclear plant. It is also a screening model that simulates remediation by natural attenuation of dissolved solvents at chlorinated solvent release sites.

It should be noted the derived analytical model still has its application limitations for that the groundwater flow in the study site is non-uniform or the site have multiple distinct zones. Furthermore, the developed model cannot simulate the more complicated decay chain problems such as diverging, converging and branched decay chains. The analytical model for more complicated decay chain problems can be pursued in the near future.

Appendix A

Derivation of analytical solutions

In this appendix, we elaborate on the mathematical procedures for deriving the analytical solutions.

The Laplace transforms of Eqs. (7a), (7b), (9)-(12) yield

$$\frac{1}{Pe_L}\frac{\partial^2 G_1(X,Y,s)}{\partial X^2}-\frac{\partial G_1(X,Y,s)}{\partial X}+\frac{\rho^2}{Pe_T}\frac{\partial^2 G_1(X,Y,s)}{\partial Y^2}-(R_1 s+\kappa_1)G_1(X,Y,s)=0 \tag{A1a}$$

$$\frac{1}{Pe_L}\frac{\partial^2 G_i(X,Y,s)}{\partial X^2}-\frac{\partial G_i(X,Y,s)}{\partial X}+\frac{\rho^2}{Pe_T}\frac{\partial^2 G_i(X,Y,s)}{\partial Y^2} \quad i=2,3,...N \tag{A1b}$$
$$-\kappa_i G_i(X,Y,s)+\kappa_{i-1}G_{i-1}(X,Y,s)=R_i s G_i(X,Y,s)$$

$$-\frac{1}{Pe_L}\frac{\partial G_i(X=0,Y,s)}{\partial X}+G_i(X=0,Y,s)=F_i(s)\left[H(Y-Y_1)-H(Y-Y_2)\right] \quad 0\le Y\le 1 \; i=1...N. \tag{A2}$$

$$\frac{\partial G_i(X=1,Y,s)}{\partial X}=0 \qquad 0\le Y\le 1 \qquad i=1...N. \tag{A3}$$

$$\frac{\partial G_i(X,Y=0,s)}{\partial Y}=0 \qquad 0\le X\le 1 \qquad i=1...N. \tag{A4}$$

$$\frac{\partial G_i(X,Y=1,s)}{\partial Y}=0 \qquad 0\le X\le 1 \qquad i=1...N. \tag{A5}$$

where s is the Laplace transform parameter, and $G_i(X,Y,s)$ and $F_i(s)$ are defined by the Laplace transformation relations as

$$G_i(X,Y,s)=\int_0^\infty e^{-sT}C_i(X,Y,T)dT \tag{A6}$$

$$F_i(s)=\int_0^\infty e^{-sT}f_i(T)dT \tag{A7}$$

The finite Fourier cosine transform is used here because it satisfies the transformed governing

390 equations in Eqs. (A1a) and (A2b) and their corresponding boundary conditions in Eqs. (A4) and (A5).

391 Application of the finite Fourier cosine transform on Eqs. (A1)-(A3) leads to

392 $$\frac{1}{Pe_L}\frac{d^2H_1(X,n,s)}{\partial X^2}-\frac{dH_1(X,n,s)}{dX}-\left(R_1 s+\kappa_1+\frac{\rho^2 n^2\pi^2}{Pe_T}\right)H_1(X,n,s)=0 \quad \text{(A8a)}$$

393 $$\frac{1}{Pe_L}\frac{d^2H_i(X,n,s)}{dX^2}-\frac{dH_i(X,n,s)}{dX}-\left(R_i s+\kappa_i+\frac{\rho^2 n^2\pi^2}{Pe_T}\right)H_i(X,n,s)+\kappa_{i-1}H_{i-1}(X,n,s)=0 \quad \text{(A8b)}$$

394 $$-\frac{1}{Pe_L}\frac{dH_i(X=0,n,s)}{dX}+H_i(X=0,n,s)=F_i(s)\Phi(n) \quad \text{(A9)}$$

395 $$\frac{dH_i(X=1,n,s)}{dX}=0 \quad \text{(A10)}$$

396 where $\Phi(n)=\begin{cases}Y_2-Y_1 & n=0\\ \dfrac{\sin(n\pi Y_2)-\sin(n\pi Y_1)}{n\pi} & n=1,2,3...\end{cases}$, n is the finite Fourier cosine transform

397 parameter, $H_i(X,n,s)$ is defined by the following conjugate equations (Sneddon, 1972)

398 $$H_i(X,n,s)=\int_0^1 G_i(X,Y,s)\cos(n\pi Y)dY \quad \text{(A11)}$$

399 $$G_i(X,Y,s)=H_i(X,n=0,s)+2\sum_{n=1}^{n=\infty}H_i(X,n,s)\cos(n\pi Y) \quad \text{(A12)}$$

400 Using changes-of-variables, similar to those applied by Chen and Liu (2011), the advective terms
401 in Eqs. (A8a) and A(8b) as well as nonhomogeneous terms in Eq. (A9) can be easily removed. Thus,
402 substitutions of the change-of-variable into Eqs. (A8a), (A8b), (A9) and (A10) result in diffusive-type
403 equations associated with homogeneous boundary conditions

404 $$\frac{1}{Pe_L}\frac{d^2U_1(X,n,s)}{dX^2}-\left(R_1 s+\kappa_1+\frac{\rho^2 n^2\pi^2}{Pe_T}+\frac{Pe_L}{4}\right)U_1(X,n,s)$$
$$=e^{-\frac{Pe_L}{2}X}\left(R_1 s+\kappa_1+\frac{\rho^2 n^2\pi^2}{Pe_T}\right)F_1(s)\Phi(n) \quad \text{(A13a)}$$

$$\frac{1}{Pe_L}\frac{d^2U_i(X,n,s)}{dX^2}-\left(\frac{Pe_L}{4}+R_i s+\kappa_1+\frac{\rho^2 n^2\pi^2}{Pe_T}\right)U_i(X,n,s)$$

$$=e^{-\frac{Pe_L}{2}X}\left(R_i s+\kappa_i+\frac{\rho^2 n^2\pi^2}{Pe_T}\right)F_i(s)\Phi(n)-e^{-\frac{Pe_L}{2}X}\kappa_{i-1}F_{i-1}(s)\Phi(n)-\kappa_{i-1}U_{i-1}(X,n,s) \quad \text{(A13b)}$$

$$-\frac{dU_i(X=0,n,s)}{dX}+\frac{Pe}{2}U_i(X=0,n,s)=0 \quad \text{(A14)}$$

$$\frac{dU_i(X=1,n,s)}{dX}+\frac{Pe_L}{2}U_i(X=1,n,s)=0 \quad \text{(A15)}$$

where $U_i(X,n,s)$ is defined as the following change-of-variable relation

$$H_i(X,n,s)=F_i(s)\Phi(n)+e^{\frac{Pe_L}{2}X}U_i(X,n,s) \quad \text{(A16)}$$

As detailed in Ozisik (1989), the generalized integral transform pairs for Eqs. (A13a) and (A13b) and its associated boundary conditions (A14) and (A15) are defined as

$$Z_i(\xi_l,n,s)=\int_0^1 K(\xi_l,X)U_i(X,n,s)dX \quad \text{(A17)}$$

$$U_i(X,n,s)=\sum_{l=1}^{\infty}\frac{K(\xi_l,X)}{N(\xi_l)}Z_i(\xi_l,n,s) \quad \text{(A18)}$$

where $K(\xi_l,X)=\frac{Pe_L}{2}\sin(\xi_l X)+\xi_l\cos(\xi_l X)$ is the kernel function, $N(\xi_l)=\frac{2}{\frac{Pe_L{}^2}{4}+Pe_L+\xi_l{}^2}$,

ξ_l is the eigenvalue, determined from the equation

$$\xi_l\cot\xi_l-\frac{\xi_l{}^2}{Pe_L}+\frac{Pe_L}{4}=0 \quad \text{(A19)}$$

The generalized integral transforms of Eqs. (13a) and (13b) give

$$-\left(R_1 s+\kappa_1+\frac{\rho^2 n^2\pi^2}{Pe_T}+\frac{Pe_L}{4}+\frac{\xi_l{}^2}{Pe_L}\right)Z_i(\xi_l,n,s)=\left(R_1 s+\kappa_1+\frac{\rho^2 n^2\pi^2}{Pe_T}\right)F_1(s)\Phi(n)\Theta(\xi_l) \quad \text{(A20)}$$

$$-\left(R_i s+\kappa_i+\frac{\rho^2 n^2 \pi^2}{Pe_T}+\frac{Pe_L}{4}+\frac{{\xi_l}^2}{Pe_L}\right)Z_i(\xi_l,n,s)$$
$$=\left(R_i s+\kappa_i+\frac{\rho^2 n^2 \pi^2}{Pe_T}\right)F_i(s)\Phi(n)\Theta(\xi_l)-\kappa_{i-1}F_{i-1}(s)\Phi(n)\Theta(\xi_l)-\kappa_{i-1}Z_{i-1}(\xi_l,n,s) \quad \text{(A21)}$$

where $\Theta(\xi_l)=\dfrac{Pe_L\xi_l}{\dfrac{{Pe_L}^2}{4}+{\xi_l}^2}$.

Solving for Eqs. (A20) and (A21) algebraically for each species, $Z_i(\xi_l,n,s)$, in sequence, leads to

$$Z_1(\xi_l,n,s)=-\frac{s+\alpha_1-\beta_1}{s+\alpha_1}F_1(s)\Phi(n)\Theta(\xi_l) \quad \text{(A22)}$$

$$Z_2(\xi_l,n,s)=\left[-\frac{s+\alpha_2-\beta_2}{s+\alpha_2}F_2(s)+\frac{\sigma_2\beta_1}{(s+\alpha_2)(s+\alpha_1)}F_1(s)\right]\Phi(n)\Theta(\xi_l) \quad \text{(A23)}$$

$$Z_3(\xi_l,n,s)=\left[-\frac{s+\alpha_3-\beta_3}{s+\alpha_3}F_3(s)+\frac{\sigma_3\beta_2}{(s+\alpha_3)(s+\alpha_2)}F_2(s)\right.$$
$$\left.\frac{\sigma_3\sigma_2\beta_1}{(s+\alpha_3)(s+\alpha_2)(s+\alpha_1)}F_1\right]\Phi(n)\Theta(\xi_l) \quad \text{(A24)}$$

$$Z_4(\xi_l,n,s)=\left[-\frac{s+\alpha_4-\beta_4}{s+\alpha_4}F_4(s)+\frac{\sigma_4\beta_3}{(s+\alpha_4)(s+\alpha_3)}F_3(s)\right.$$
$$\left.+\frac{\sigma_4\sigma_3\beta_2}{(s+\alpha_4)(s+\alpha_3)(s+\alpha_2)}F_2(s)+\frac{\sigma_4\sigma_3\sigma_2\beta_1}{(s+\alpha_4)(s+\alpha_3)(s+\alpha_2)(s+\alpha_1)}F_1(s)\right]\Phi(n)\Theta(\xi_l) \quad \text{(A25)}$$

where $\alpha_i(\xi_l)=\dfrac{\kappa_i}{R_i}+\dfrac{\rho^2 n^2\pi^2}{Pe_T R_i}+\dfrac{Pe_L}{4R_i}+\dfrac{{\xi_l}^2}{Pe_L R_i}$, $\beta_i(\xi_l)=\dfrac{Pe_L}{4R_i}+\dfrac{{\xi_l}^2}{Pe_L R_i}$, $\sigma_i=\dfrac{\kappa_{i-1}}{R_i}$.

Upon inspection of Eqs. (A22)-(A25), compact expressions valid for all species can be generalized as

$$Z_i(\xi_l,n,s)=\left[P_i(\xi_l,n,s)+Q_i(\xi_l,n,s)\right]\Phi(n)\Theta(\xi_l) \quad i=1,2...N \quad \text{(A26)}$$

where $P_i(\xi_l,n,s) = -\dfrac{s+\alpha_i-\beta_i}{s+\alpha_i}F_i(s)$ and $Q_i(\xi_l,n,s) = \sum_{k=0}^{k=i-2} \dfrac{\beta_{i-k-1}\prod_{j_1=0}^{j_1=k}\sigma_{i-j_1}}{\prod_{j_2=0}^{j_2=k+1}\left(s+\alpha_{i-j_2}\right)}F_{i-k-1}(s)$.

The solutions in the original domain are obtained by a series of integral transform inversions in combination with changes-of-variables.

The inverse generalized integral transform of Eq. (A26) gives

$$W_i(X,n,s) = \sum_{m=1}^{\infty}\frac{K(\xi_l,X)}{N(\xi_l)}\left[P_i(\xi_l,n,s)+Q_i(\xi_l,n,s)\right]\Phi(n)\Theta(\xi_l) \tag{A27}$$

Using change-of-variable relation of Eq. (A16), one obtains

$$H_i(\xi_l,n,s) = F_i(s)\Phi(n) + e^{\frac{Pe_L}{2}x_D}\sum_{m=1}^{\infty}\frac{K(\xi_l,x_D)}{N(\xi_l)}\left[P_i(\xi_l,n,s)+Q_i(\xi_l,n,s)\right]\Phi(n)\Theta(\xi_l) \tag{A28}$$

The finite Fourier cosine inverse transform of Eq. (A28) results in

$$\begin{aligned} &G_i(X,Y,s) \\ &= F_i(s)\Phi(n=0) + e^{\frac{Pe_L}{2}X}\cdot\sum_{l=1}^{\infty}\frac{K(\xi_l,X)}{N(\xi_l)}\left[P_i(\xi_l,n,s)+Q_i(\xi_l,n,s)\right]\Phi(n=0)\Theta(\xi_l) \\ &+2\sum_{n=1}^{n=\infty}\left\{F_i(s)\Phi(n)+e^{\frac{Pe_L}{2}X}\sum_{l=1}^{\infty}\frac{K(\xi_l,X)}{N(\xi_l)}\left[P_i(\xi_l,n,s)+Q_i(\xi_l,n,s)\right]\Phi(n)\Theta(\xi_l)\right\}\cos(n\pi Y) \end{aligned} \tag{A29}$$

The analytical solutions in the original domain will be completed by taking the Laplace inverse transform of Eq. (A29). $P_i(\xi_l,n,s)$ in Eq. (29) is in the form of the product of two functions . The Laplace transform of $\dfrac{s+\alpha_i-\beta_i}{s+\alpha_i}$ can be easily obtained as

$$L^{-1}\left[\frac{s+\alpha_i-\beta_i}{s+\alpha_i}\right] = \delta(T) - \beta_i e^{-\alpha_i T} \tag{A30}$$

Thus, the Laplace inverse of $P_i(\xi_l,n,s)$ can be achieved using the convolution theorem as

444 $$p_i(\xi_l, n, T) = L^{-1}\left[P_i(\xi_l, n, s)\right] = L^{-1}\left[-\frac{s+\alpha_i-\beta_i}{s+\alpha_i}F_i(s)\right] = -f_i(T) + \beta_i e^{-\alpha_i T}\int_0^T f_i(\tau)e^{\alpha_i \tau}d\tau \qquad \text{(A31)}$$

445 The Laplace inverse of $Q_i(\xi_l, n, s)$ can be also approached using the similar method. By taking

446 Laplace inverse transform on $Q_i(\xi_l, n, s)$, we have

447 $$q_i(\xi_l, n, T) = L^{-1}\left[Q_i(\xi_l, n, s)\right] = L^{-1}\left[\sum_{k=0}^{k=i-2}\frac{\beta_{i-k-1}\prod_{j_1=0}^{j_1=k}\sigma_{i-j_1}}{\prod_{j_2=0}^{j_2=k+1}\left(s+\alpha_{i-j_2}\right)}F_{i-k-1}(s)\right]$$

448 $$= \sum_{k=0}^{k=i-2}\beta_{i-k-1}\prod_{j_1=0}^{j_1=k}\sigma_{i-j_1}L^{-1}\left[\frac{1}{\prod_{j_2=0}^{j_2=k+1}\left(s+\alpha_{i-j_2}\right)}F_{i-k-1}(s)\right] \qquad \text{(A32)}$$

449

450 Expressing $\frac{1}{\prod_{j_2=0}^{j_2=k+1}\left(s+\alpha_{i-j_2}\right)}$ as the summation of partial fractions and applying the inverse

451 Laplace transform formula, one gets

452 $$L^{-1}\left[\frac{1}{\prod_{j_2=0}^{j_2=k+1}\left(s+\alpha_{i-j_2}\right)}\right] = L^{-1}\left[\sum_{j_2=0}^{j_2=k+1}\frac{1}{\prod_{j_3=i-k-1, j_3\neq i-j_2}^{j_3=i}(\alpha_{j_3}-\alpha_{i-j_2})\left(s+\alpha_{i-j_2}\right)}\right]$$

453 $$= \sum_{j_2=0}^{j_2=k+1}\frac{e^{-\alpha_{i-j_1}T}}{\prod_{j_3=i-k-1, j_3\neq i-j_1}^{j_3=i}(\alpha_{j_3}-\alpha_{i-j_1})} \qquad \text{(A33)}$$

454

455 Recall that the inverse Laplace transform of $F_{i-k-1}(s)$ is $f_{i-k-1}(T)$. Thus, the Laplace inverse

transform of $\frac{1}{\prod_{j_2=0}^{j_2=k+1}\left(s+\alpha_{i-j_2}\right)}F_{i-k-1}(s)$ in Eq. (1) can be achieved using the convolution integral equation as

$$L^{-1}\left[\frac{1}{\prod_{j_2=0}^{j_2=k+1}\left(s+\alpha_{i-j_2}\right)}F_{i-k-1}(s)\right]=\sum_{j_2=0}^{j_2=k+1}\frac{e^{-\alpha_{i-j_1}T}\int_0^T e^{\alpha_{i-j_1}\tau}f_{i-k-1}(\tau)d\tau}{\prod_{j_3=i,\ j_3=i-k-1,\ j_3\neq i-j_2}^{j_3=i}\left(\alpha_{j_3}-\alpha_{i-j_2}\right)} \tag{A34}$$

Putting Eq. (A34) into Eq. (A2) we can obtain the following form:

$$q_i(\xi_l,n,T)=\sum_{k=0}^{k=i-2}\beta_{i-k-1}\prod_{j_1=0}^{j_1=k}\sigma_{i-j_1}\sum_{j_2=0}^{j_2=k+1}\frac{e^{-\alpha_{i-j_1}T}\int_0^T e^{\alpha_{i-j_1}\tau}f_{i-k-1}(\tau)d\tau}{\prod_{j_3=i,\ j_3=i-k-1,\ j_3\neq i-j_2}^{j_3=i}\left(\alpha_{j_3}-\alpha_{i-j_2}\right)} \tag{A35}$$

Thus, the final solution can be expressed as Eq.(13) with the corresponding functions defined in Eqs.(14) and (15).

Note that Eq. (A33) is invalid for some of α_{i-j_2} being identical. For such conditions, we can still reduce $\frac{1}{\prod_{j_2=0}^{j_2=k+1}\left(s+\alpha_{i-j_2}\right)}$ to a sum of partial fraction expansion. However, it will lead to different Laplace inverse formulae. For example, the following formulae is used for all α_{i-j_2} being identical

$$L^{-1}\left[\frac{1}{\prod_{j_2=0}^{j_2=k+1}\left(s+\alpha_{i-j}\right)}\right]=\frac{T^k e^{-\alpha_{i-j_2}T}}{k!} \tag{A36}$$

The generalized formulae for the cases with some of α_{i-j_2} being identical will not be provided

herein because there are a large number of combinations of α_{i-j_2}. We suggest that the readers can pursue the solutions by following the similar steps for such specific conditions case by case.

Acknowledgement

The authors are grateful to the Ministry of Science and Technology, Republic of China, for financial support of this research under contract MOST 103-2221-E-0008-100. The authors thanks three anonymous referees for their helpful comments and suggestions.

References

Aziz, C. E., Newell, C. J., Gonzales, J. R., Haas P., Clement, T. P., Sun, Y.: BIOCHLOR—Natural attenuation decision support system v1.0, User's Manual, U.S. EPA Report, EPA 600/R-00/008, 2000.

Barry, D. A., Sposito, G.: Application of the convection-dispersion model to solute transport in finite soil columns, Soil Sc. Soc. Am. J., 52, 3-9, 1988.

Batu, V.: A generalized two-dimensional analytical solution for hydrodynamic dispersion in bounded media with the first-type boundary condition at the source, Water Resour. Res., 25, 1125-1132, 1989.

Batu, V.: A generalized two-dimensional analytical solute transport model in bounded media for flux-type finite multiple sources, Water Resour. Res., 29, 2881-2892, 1993.

Batu, V.: A generalized three-dimensional analytical solute transport model for multiple rectangular first-type sources, J. Hydrol. 174, 57-82, 1996.

Bauer, P., Attinger, S., Kinzelbach, W.: Transport of a decay chain in homogeneous porous media: analytical solutions, J. Contam. Hydrol. 49, 217-239, 2001.

492 Chen, J. S., Liu, C. W.: Generalized analytical solution for advection-dispersion equation in finite
493 spatial domain with arbitrary time-dependent inlet boundary condition, Hydrol. Earth Sys. Sci.,
494 15, 2471-2479, 2011.
495 Chen, J. S., Ni, C. F., Liang, C. P., Chiang, C. C.: Analytical power series solution for contaminant
496 transport with hyperbolic asymptotic distance-dependent dispersivity, J. Hydrol., 362, 142-149,
497 2008a.
498 Chen, J. S., Ni, C. F., Liang, C. P.: Analytical power series solutions to the two-dimensional advection-
499 dispersion equation with distance-dependent dispersivities, Hydrol. Process., 22, 670-4678,
500 2008b.
501 Chen, J. S., Chen, J. T., Liu, C. W., Liang, C. P., Lin, C. M.: Analytical solutions to two-dimensional
502 advection–dispersion equation in cylindrical coordinates in finite domain subject to first- and
503 third-type inlet boundary conditions, J. Hydrol., 405, 522-531, 2011.
504 Chen, J. S., Lai, K. H., Liu, C. W., Ni, C. F.: A novel method for analytically solving multi-species
505 advective-dispersive transport equations sequentially coupled with first-order decay reactions.
506 J. Hydrol., 420-421, 191-204, 2012a.
507 Chen, J. S., Liu, C. W., Liang, C. P., Lai, K. H.: Generalized analytical solutions to sequentially
508 coupled multi-species advective-dispersive transport equations in a finite domain subject to an
509 arbitrary time-dependent source boundary condition, J. Hydrol., 456-457, 101-109, 2012b.
510 Cho C. M.: Convective transport of ammonium with nitrification in soil, Can. J. Soil Sci., 51, 339-350,
511 1971.
512 Clement, T. P.: Generalized solution to multispecies transport equations coupled with a first-order
513 reaction-network, Water Resour. Res., 37, 157-163, 2001.

514 Gao, G., Zhan, H., Feng, S., Fu, B., Ma, Y., Huang, G.: A new mobile-immobile model for reactive
515 solute transport with scale-dependent dispersion, Water Resour. Res., 46, W08533
516 doi:10.1029/2009WR008707, 2010.
517 Gao, G., Zhan, H., Feng, S., Huang, G., Fu, B.: A mobile-immobile model with an asymptotic scale-
518 dependent dispersion function, J. Hydrol., 424-425, 172-183, 2012.
519 Gao, G., Fu, B., Zhan, H., Ma, Y.: Contaminant transport in soil with depth-dependent reaction
520 coefficients and time-dependent boundary conditions, Water Res., 47, 2507-2522, 2013.
521 Higashi, K., Pigford, T.: Analytical models for migration of radionuclides in geological sorbing media,
522 J. Nucl. Sci. Technol., 17(10), 700-709, 1980.
523 Leij, F. J., Skaggs, T. H., Van Genuchten, M. Th.: Analytical solution for solute transport in three-
524 dimensional semi-infinite porous media, Water Resour. Res., 27, 2719-2733, 1991.
525 Leij, F. J., Toride, N., van Genuchten, M.Th.: Analytical solutions for non-eq uilibrium solute transport
526 in three-dimensional porous media, J. Hydrol., 151, 193-228, 1993.
527 Lunn, M., Lunn. R.J., Mackay, R.: Determining analytic solution of multiple species contaminant
528 transport with sorption and decay, J. Hydrol., 180, 195-210, 1996.
529 McGuire, T. M., Newell, C. J., Looney, B. B., Vangeas, K. M., Sink, C. H., 2004: Historical analysis
530 of monitored natural attenuation: A survey of 191 chlorinated solvent site and 45 solvent
531 plumes. Remiat. J. 15: 99-122.
532 Mieles J, Zhan H.: Analytical solutions of one-dimensional multispecies reactive transport in a
533 permeable reactive barrier-aquifer system, J. Contam. Hydrol., 134-135, 54-68, 2012.
534 Montas, H. J.: An analytical solution of the three-component transport equation with application to
535 third-order transport, Water Resour. Res., 39, 1036 doi:10.1029/2002WR00128, 2003.
536 Moridis, G. J., Reddell, D. L.: The Laplace transform finite difference method for simulation of flow
537 through porous media, Water Resour. Res., 27, 1873-1884, 1991.

538 Ozisik, M. N.: Boundary Value Problems of Heat Conduction, Dover Publications, Inc., New York,
539 1989.
540 Parlange, J. Y., Starr, J. L., van Genuchten, M. Th., Barry, D. A., Parker, J. C.: Exit condition for
541 miscible displacement experiments in finite columns, Soil Sci., 153, 165-171, 1992.
542 Park, E., Zhan, H.: Analytical solutions of contaminant transport from finite one-, two, three-
543 dimensional sources in a finite-thickness aquifer, J. Contam. Hydrol., 53, 41-61, 2000.
544 Pérez Guerrero, J. S., Skaggs, T. H.: Analytical solution for one-dimensional advection-dispersion
545 transport equation with distance-dependent coefficients, J. Hydrol., 390, 57-65, 2010.
546 Pérez Guerrero, J. S., Pimentel, L. G. G., Skaggs, T. H., van Genuchten, M. Th.: Analytical solution
547 for multi-species contaminant transport subject to sequential first-order decay reactions in finite
548 media, Transport in Porous Med., 80, 357–373, 2009.
549 Pérez Guerrero, J. S., Skaggs, T. H., van Genuchten, M. Th., Analytical solution for multi-species
550 contaminant transport in finite media with time-varying boundary condition, Transport Porous
551 Med., 85, 171-188, 2010.
552 Pérez Guerrero, J. S., Pontedeiro, E. M., van Genuchten, M. Th., Skaggs, T. H. : Analytical solutions
553 of the one-dimensional advection–dispersion solute transport equation subject to time-
554 dependent boundary conditions, Chem. Eng. J., 221, 487-491, 2013.
555 Quezada, C. R., Clement, T. P., Lee, K. K.: Generalized solution to multi-dimensional multi-species
556 transport equations coupled with a first-order reaction network involving distinct retardation
557 factors, Adv. Water Res., 27, 507-520, 2004.
558 Sneddon, I. H.: The Use of Integral Transforms, McGraw-Hill, New York, 1972.
559 Srinivasan, V., Clememt, T. P.: Analytical solutions for sequentially coupled one-dimensional reactive
560 transport problems-Part I: Mathematical derivations, Adv. Water Resour., 31, 203-218, 2008a.
561 Srinivasan, V., Clememt, T. P.: Analytical solutions for sequentially coupled one-dimensional reactive

transport problems-Part II: Special cases, implementation and testing, Advances in Water Resour. 31, 219-232, 2008b.

Sudicky, E. A., Hwang, H. T., Illman, W. A., Wu, Y. S.: A semi-analytical solution for simulating contaminant transport subject to chain-decay reactions, J. Contam. Hydrol., 144, 20-45, 2013.

Sun, Y., Clement, T. P.: A decomposition method for solving coupled multi-species reactive transport problems, Transport in Porous Med., 37, 327-346, 1999.

Sun, Y., Peterson, J. N., Clement, T. P.: A new analytical solution for multiple species reactive transport in multiple dimensions, J. Contam. Hydrol., 35, 429-440, 1999a.

Sun, Y., Petersen, J. N., Clement, T. P., Skeen, R. S.: Development of analytical solutions for multi-species transport with serial and parallel reactions, Water Resour. Res., 35, 185-190, 1999b.

van Genuchten, M.Th., Alves, W. J.: Analytical solutions of the one-dimensional convective-dispersive solute transport equation, US Department of Agriculture Technical Bulletin No. 1661, 151pp, 1982.

van Genuchten, M.Th.: Convective–dispersive transport of solutes involved in sequential first-order decay reactions, Comput. Geosci., 11, 129–147, 1985.

Yeh, G.T.: AT123D: Analytical Transient One-, Two-, and Three-Dimensional Simulation of Waste Transport in the Aquifer System. ORNL-5602, Oak Ridge National Laboratory, 1981.

Zhan, H., Wen, Z., Gao, G.: An analytical solution of two-dimensional reactive solute transport in an aquifer–aquitard system. Water Resources Research 45, W10501. doi:10.1029/2008WR007479, 2009.

Ziskind, G., Shmueli, H., Gitis, V.: An analytical solution of the convection–dispersion–reaction equation for a finite region with a pulse boundary condition, Chem. Eng. J., 167, 403-408, 2011.

Table 1

Transport parameters used for convergence test example 1 involving the four-species radionuclide decay chain problem used by van Genuchten (1985)

Parameter	Value
Domain length, L [m]	250
Domain width, W [m]	100
Seepage velocity, v [m year^{-1}]	100
Longitudinal Dispersion coefficient, D_L [m^2 year^{-1}]	1,000
Transverse Dispersion coefficient, D_T [m^2 year^{-1}]	100
Retardation coefficient, R_i	
^{238}Pu	10,000
^{234}U	14,000
^{230}Th	50,000
^{226}Ra	500
Decay constant, k_i [year^{-1}]	
^{238}Pu	0.0079
^{234}U	0.0000028
^{230}Th	0.0000087
^{226}Ra	0.00043
Source decay constant, λ_m [year^{-1}]	
^{238}Pu	0.0089
^{234}U	0.00100280
^{230}Th	0.00100870
^{226}Ra	0.00143

Table 2

Values for coefficients of Bateman-type boundary source for four-species transport problem used by van Genuchten (1985)

Species, *i*	b_{im}			
	m=1	*m=2*	*m=3*	*m=4*
^{238}Pu , *i=1*	1.25			
^{234}U , *i=2*	-1.25044	1.25044		
^{230}Th , *i=3*	0.443684×10^{-3}	0.593431	-0.593874	
^{226}Ra , *i=4*	-0.516740×10^{-6}	0.120853×10^{-1}	-0.122637×10^{-1}	0.178925×10^{-3}

Table 3

Solution convergence of each species concentration at transect of inlet boundary ($x = 0$) for four-species radionuclide transport problem considering simulated domain of $L = 250$ m, $W = 100$ m, subject to Bateman-type sources located at $40\,m \le y \le 60\,m$ for t = 1,000 year (M = number of terms summed for inverse generalized integral transform; N = number of terms summed for inverse finite Fourier cosine transform). When we investigate the required M for inverse generalized integral transform, N=16,000 for the finite Fourier cosine transform inverse are used. When we investigate the required N for inverse finite Fourier cosine transform, M=1,600 for the generalized transform inverse are used.

^{238}Pu

x [m]	y [m]	M =100	M =200	M =400	M =800	M =1,600
0	30	2.714E-07	2.712E-07	2.711E-07	2.710E-07	2.710E-07
0	34	3.412E-06	3.412E-06	3.411E-06	3.411E-06	3.411E-06
0	38	2.677E-05	2.677E-05	2.677E-05	2.677E-05	2.677E-05
0	46	1.608E-04	1.609E-04	1.609E-04	1.609E-04	1.609E-04
0	50	1.637E-04	1.637E-04	1.637E-04	1.637E-04	1.637E-04
x [m]	y [m]	N =1,000	N =2,000	N =4,000	N =8,000	N =16,000
0	30	2.723E-07	2.713E-07	2.711E-07	2.710E-07	2.710E-07
0	34	3.413E-06	3.412E-06	3.411E-06	3.411E-06	3.411E-06
0	38	2.677E-05	2.677E-05	2.677E-05	2.677E-05	2.677E-05
0	46	1.609E-04	1.609E-04	1.609E-04	1.609E-04	1.609E-04
0	50	1.637E-04	1.637E-04	1.637E-04	1.637E-04	1.637E-04

^{234}U

x [m]	y [m]	M =25	M =50	M =100	M =200	M =400
0	32	1.092E-03	1.091E-03	1.090E-03	1.090E-03	1.090E-03
0	34	4.829E-03	4.827E-03	4.826E-03	4.826E-03	4.825E-03
0	38	5.745E-02	5.753E-02	5.753E-02	5.753E-02	5.753E-02
0	46	3.999E-01	4.004E-01	4.005E-01	4.005E-01	4.005E-01
0	50	4.044E-01	4.049E-01	4.049E-01	4.049E-01	4.049E-01
x [m]	y [m]	N =500	N =1,000	N =2,000	N =4,000	N =8,000
0	32	1.107E-03	1.094E-03	1.091E-03	1.090E-03	1.090E-03
0	34	4.850E-03	4.831E-03	4.827E-03	4.826E-03	4.825E-03
0	38	5.761E-02	5.755E-02	5.753E-02	5.753E-02	5.752E-02

0	46	4.0005E-01	4.005E-01	4.005E-01	4.005E-01	4.005E-01
0	50	4.049E-01	4.049E-01	4.049E-01	4.049E-01	4.049E-01

608 ^{230}Th

x [m]	y [m]	M =100	M =200	M =400	M =800	M =1,600
0	34	1.498E-06	1.495E-06	1.493E-06	1.492E-06	1.492E-06
0	38	4.269E-05	4.267E-05	4.267E-05	4.266E-05	4.266E-05
0	42	6.847E-04	6.848E-04	6.848E-04	6.848E-04	6.848E-04
0	46	7.259E-04	7.260E-04	7.260E-04	7.260E-04	7.260E-04
0	50	7.273E-04	7.274E-04	7.274E-04	7.274E-04	7.274E-04
x [m]	y [m]	N =1,000	N =2,000	N =4,000	N =8,000	N =16,000
0	34	1.514E-06	1.497E-06	1.493E-06	1.492E-06	1.492E-06
0	38	4.274E-05	4.268E-05	4.267E-05	4.266E-05	4.266E-05
0	42	6.847E-04	6.848E-04	6.848E-04	6.848E-04	6.848E-04
0	46	7.259E-04	7.260E-04	7.260E-04	7.260E-04	7.260E-04
0	50	7.274E-04	7.274E-04	7.274E-04	7.274E-04	7.274E-04

609 ^{226}Ra

x [m]	y [m]	M =50	M =100	M =200	M =400	M =800
0	18	3.084E-08	3.082E-08	3.082E-08	3.081E-08	3.081E-08
0	24	1.294E-07	1.293E-07	1.293E-07	1.293E-07	1.293E-07
0	28	3.492E-07	3.492E-07	3.492E-07	3.492E-07	3.492E-07
0	44	2.217E-05	2.222E-05	2.223E-05	2.223E-05	2.223E-05
0	50	2.425E-05	2.430E-05	2.431E-05	2.431E-05	2.431E-05
x [m]	y [m]	N =1,000	N =2,000	N =4,000	N =8,000	N =16,000
0	18	3.086E-08	3.082E-08	3.082E-08	3.081E-08	3.081E-08
0	24	1.294E-07	1.293E-07	1.293E-07	1.293E-07	1.293E-07
0	28	3.493E-07	3.492E-07	3.492E-07	3.492E-07	3.492E-07
0	44	2.223E-05	2.223E-05	2.223E-05	2.223E-05	2.223E-05
0	50	2.431E-05	2.431E-05	2.431E-05	2.431E-05	2.431E-05

610

611

612

Table 4

Solution convergence of each species concentration at transect of $x = 25$ m for four-species radionuclide transport problem considering simulated domain of $L = 250$ m, $W = 100$ m, subject to Bateman-type sources located at $40\,m \le y \le 60\,m$ for t = 1,000 year (M = number of terms summed for inverse generalized integral transform; N = number of terms summed for inverse finite Fourier cosine transform). When we investigate the required M for inverse generalized integral transform, N=160 for the finite Fourier cosine transform inverse are used. When we investigate the required N for inverse finite Fourier cosine transform, M=1,600 for the generalized transform inverse are used.

^{238}Pu

x [m]	y [m]	M =100	M =200	M =400	M =800	M =1,600
25	28	5.531E-08	5.576E-08	5.580E-08	5.580E-08	5.580E-08
25	30	2.319E-07	2.312E-07	2.312E-07	2.311E-07	2.311E-07
25	38	1.106E-05	1.106E-05	1.106E-05	1.106E-05	1.106E-05
25	46	3.430E-05	3.430E-05	3.430E-05	3.430E-05	3.430E-05
25	50	3.616E-05	3.616E-05	3.616E-05	3.616E-05	3.616E-05
x [m]	y [m]	N =10	N =20	N =40	N =80	N =160
25	28	-7.841E-07	9.961E-08	5.579E-08	5.580E-08	5.580E-08
25	30	-4.063E-07	2.616E-07	2.312E-07	2.311E-07	2.311E-07
25	38	1.195E-05	1.114E-05	1.106E-05	1.106E-05	1.106E-05
25	46	3.404E-05	3.441E-05	3.430E-05	3.430E-05	3.430E-05
25	50	3.817E-05	3.606E-05	3.616E-05	3.616E-05	3.616E-05

^{234}U

x [m]	y [m]	M =100	M =200	M =400	M =800	M =1,600
25	30	9.734E-05	9.612E-05	9.594E-05	9.592E-05	9.592E-05
25	34	1.727E-03	1.725E-03	1.724E-03	1.724E-03	1.724E-03
25	38	1.167E-02	1.167E-02	1.167E-02	1.167E-02	1.167E-02
25	46	4.023E-02	4.024E-02	4.024E-02	4.024E-02	4.024E-02
25	50	4.177E-02	4.178E-02	4.178E-02	4.178E-02	4.178E-02
x [m]	y [m]	N =10	N =20	N =40	N =80	N =160
25	30	-9.427E-04	1.728E-04	9.610E-05	9.592E-05	9.592E-05
25	34	3.154E-03	1.588E-03	1.725E-03	1.724E-03	1.724E-03
25	38	1.324E-02	1.186E-02	1.167E-02	1.167E-02	1.167E-02

25	46	3.984E-02	4.049E-02	4.024E-02	4.024E-02	4.024E-02
25	50	4.487E-02	4.153E-02	4.178E-02	4.178E-02	4.178E-02

624

625 ^{230}Th

x [m]	y [m]	M =100	M =200	M =400	M =800	M =1,600
25	30	1.822E-08	1.379E-08	1.312E-08	1.305E-08	1.305E-08
25	34	3.288E-07	3.207E-07	3.195E-07	3.193E-07	3.193E-07
25	38	2.766E-06	2.740E-06	2.735E-06	2.735E-06	2.735E-06
25	46	1.013E-05	1.015E-05	1.015E-05	1.015E-05	1.015E-05
25	50	1.043E-05	1.045E-05	1.045E-05	1.045E-05	1.045E-05
x [m]	y [m]	N =10	N =20	N =40	N =80	N =160
25	30	-2.948E-07	4.484E-08	1.320E-08	1.305E-08	1.305E-08
25	34	7.000E-07	2.632E-07	3.196E-07	3.193E-07	3.193E-07
25	38	3.246E-06	2.816E-06	2.735E-06	2.735E-06	2.735E-06
25	46	1.005E-05	1.025E-05	1.015E-05	1.015E-05	1.015E-05
25	50	1.134E-05	1.035E-05	1.045E-05	1.045E-05	1.045E-05

626 ^{226}Ra

x [m]	y [m]	M =25	M =50	M =100	M =200	M =400
25	10	2.681E-08	2.757E-08	2.767E-08	2.765E-08	2.765E-08
25	14	6.580E-08	6.665E-08	6.676E-08	6.674E-08	6.674E-08
25	18	1.606E-07	1.615E-07	1.617E-07	1.617E-07	1.617E-07
25	42	1.686E-05	1.658E-05	1.656E-05	1.656E-05	1.656E-05
25	50	2.315E-05	2.278E-05	2.277E-05	2.277E-05	2.277E-05
x [m]	y [m]	N =10	N =20	N =40	N =80	N =160
25	10	-5.355E-08	3.027E-08	2.766E-08	2.765E-08	2.765E-08
25	14	7.068E-08	6.392E-08	6.675E-08	6.674E-08	6.674E-08
25	18	2.642E-07	1.640E-07	1.617E-07	1.617E-07	1.617E-07
25	42	1.624E-05	1.655E-05	1.656E-05	1.656E-05	1.656E-05
25	50	2.311E-05	2.275E-05	2.277E-05	2.277E-05	2.277E-05

627

628

Table 5

Solution convergence of each species concentration at transect of exit boundary ($x = 250$ m) for four-species radionuclide transport problem considering simulated domain of $L = 250$ m, $W = 100$ m subject to Bateman-type sources located at $40\,m \le y \le 60\,m$ for t = 1000 year (M = number of terms summed for inverse generalized integral transform and N = number of terms summed for inverse finite Fourier cosine transform). When we investigate the required M for inverse generalized integral transform, N=16 for the finite Fourier cosine transform inverse are used. When we investigate the required N for inverse finite Fourier cosine transform, M=6,400 for the generalized transform inverse are used.

^{226}Ra

x [m]	y [m]	M =400	M =800	M =1,600	M =3,200	M =6,400
250	2	2.289E-08	1.842E-08	1.814E-08	1.812E-08	1.812E-08
250	14	5.617E-08	5.060E-08	5.025E-08	5.022E-08	5.022E-08
250	26	1.528E-07	1.420E-07	1.413E-07	1.413E-07	1.413E-07
250	38	3.757E-07	2.743E-07	2.678E-07	2.674E-07	2.674E-07
250	50	1.645E-07	3.208E-07	3.306E-07	3.312E-07	3.312E-07
x [m]	y [m]	N =1	N =2	N =4	N =8	N =16
250	2	1.529E-07	-1.848E-09	1.892E-08	1.812E-08	1.812E-08
250	14	1.529E-07	5.348E-08	4.946E-08	5.022E-08	5.022E-08
250	26	1.529E-07	1.627E-07	1.414E-07	1.413E-07	1.413E-07
250	38	1.529E-07	2.666E-07	2.680E-07	2.674E-07	2.674E-07
250	50	1.529E-07	3.089E-07	3.303E-07	3.312E-07	3.312E-07

Table 6

Solution convergence of each species concentration at transect of inlet boundary ($x = 0$ m) for four-species radionuclide transport problem considering simulated domain of $L = 2{,}500$ m, $W = 100$ m subject to Bateman-type sources located at $45\,m \le y \le 55\,m$ for t = 1,000 year (M = number of terms summed for inverse generalized integral transform; N = number of terms summed for inverse finite Fourier cosine transform). When we investigate the required M for inverse generalized integral transform, N=12,800 for the finite Fourier cosine transform inverse are used. When we investigate the required N for inverse finite Fourier cosine transform, M=6,400 for the generalized transform inverse are used.

^{238}Pu

x [m]	y [m]	M =400	M =800	M =1,600	M =3,200	M =6,400
0	36	5.395E-07	5.391E-07	5.389E-07	5.387E-07	5.387E-07
0	38	1.908E-06	1.908E-06	1.908E-06	1.907E-06	1.907E-06
0	42	1.640E-05	1.642E-05	1.642E-05	1.642E-05	1.642E-05
0	46	1.203E-04	1.199E-04	1.198E-04	1.198E-04	1.198E-04
0	50	1.522E-04	1.524E-04	1.525E-04	1.525E-04	1.525E-04
x [m]	y [m]	N =2,000	N =4,000	N =8,000	N =16,000	N =32,000
0	36	5.392E-07	5.389E-07	5.388E-07	5.387E-07	5.387E-07
0	38	1.908E-06	1.908E-06	1.907E-06	1.907E-06	1.907E-06
0	42	1.642E-05	1.642E-05	1.642E-05	1.642E-05	1.642E-05
0	46	1.198E-04	1.198E-04	1.198E-04	1.198E-04	1.199E-04
0	50	1.525E-04	1.525E-04	1.525E-04	1.525E-04	1.525E-04

^{234}U

x [m]	y [m]	M =800	M =1,600	M =3,200	M =6,400	M =12,800
0	36	4.817E-04	4.815E-04	4.815E-04	4.814E-04	4.814E-04
0	38	2.348E-03	2.348E-03	2.348E-03	2.348E-03	2.348E-03
0	44	1.011E-01	1.012E-01	1.012E-01	1.012E-01	1.012E-01
0	48	3.704E-01	3.705E-01	3.705E-01	3.705E-01	3.705E-01
0	50	3.862E-01	3.864E-01	3.864E-01	3.864E-01	3.864E-01
x [m]	y [m]	N =4,000	N =8,000	N =16,000	N =32,000	N =64,000
0	36	4.818E-04	4.816E-04	4.815E-04	4.814E-04	4.814E-04
0	38	2.348E-03	2.348E-03	2.348E-03	2.348E-03	2.348E-03

0	44	1.013E-01	1.013E-01	1.012E-01	1.012E-01	1.012E-01
0	48	3.705E-01	3.705E-01	3.705E-01	3.705E-01	3.705E-01
0	50	3.864E-01	3.864E-01	3.864E-01	3.864E-01	3.864E-01

654 ^{230}Th

x [m]	y [m]	M =400	M =800	M =1,600	M =3,200	M =6,400
0	40	3.429E-06	3.427E-06	3.424E-06	3.423E-06	3.423E-06
0	42	1.773E-05	1.783E-05	1.782E-05	1.782E-05	1.782E-05
0	44	1.028E-04	1.089E-04	1.093E-04	1.093E-04	1.093E-04
0	48	7.095E-04	7.089E-04	7.090E-04	7.090E-04	7.090E-04
0	50	7.210E-04	7.205E-04	7.206E-04	7.206E-04	7.206E-04
x [m]	y [m]	N =2,000	N =4,000	N =8,000	N =16,000	N =32,000
0	40	3.430E-06	3.425E-06	3.424E-06	3.423E-06	3.423E-06
0	42	1.783E-05	1.782E-05	1.782E-05	1.782E-05	1.782E-05
0	44	1.093E-04	1.093E-04	1.093E-04	1.093E-04	1.093E-04
0	48	7.090E-04	7.090E-04	7.090E-04	7.090E-04	7.090E-04
0	50	7.206E-04	7.206E-04	7.206E-04	7.206E-04	7.206E-04

655 ^{226}Ra

x [m]	y [m]	M =400	M =800	M =1,600	M =3,200	M =6,400
0	24	3.557E-08	3.556E-08	3.556E-08	3.555E-08	3.555E-08
0	28	9.276E-08	9.274E-08	9.273E-08	9.273E-08	9.273E-08
0	40	2.159E-06	2.159E-06	2.159E-06	2.159E-06	2.159E-06
0	44	7.739E-06	7.809E-06	7.813E-06	7.813E-06	7.813E-06
0	50	2.072E-05	2.082E-05	2.083E-05	2.084E-05	2.084E-05
x [m]	y [m]	N =1,000	N =2,000	N =4,000	N =8,000	N =16,000
0	24	3.559E-08	3.557E-08	3.556E-08	3.555E-08	3.555E-08
0	28	9.278E-08	9.275E-08	9.274E-08	9.273E-08	9.273E-08
0	40	2.159E-06	2.159E-06	2.159E-06	2.159E-06	2.159E-06
0	44	7.815E-06	7.814E-06	7.813E-06	7.813E-06	7.813E-06
0	50	2.084E-05	2.084E-05	2.084E-05	2.084E-05	2.084E-05

656

657

Table 7

Solution convergence of each species concentration at transect of $x = 250$ m for four-species radionuclide transport problem considering simulated domain of $L = 2{,}500$ m, $W = 100$ m subject to Bateman-type sources located at $45\,m \le y \le 55\,m$ for t = 1,000 year (M = number of terms summed for inverse generalized integral transform; N = number of terms summed for inverse finite Fourier cosine transform). When we investigate the required M for inverse generalized integral transform, N=160 for the finite Fourier cosine transform inverse are used. When we investigate the required N for inverse finite Fourier cosine transform, M=12,800 for the generalized transform inverse are used.

^{238}Pu

x [m]	y [m]	M =200	M =400	M =800	M =1,600	M =3,200
25	32	2.578E-08	2.569E-08	2.564E-08	2.563E-08	2.563E-08
25	34	1.153E-07	1.162E-07	1.161E-07	1.161E-07	1.161E-07
25	40	3.485E-06	3.661E-06	3.661E-06	3.661E-06	3.661E-06
25	46	2.262E-05	2.176E-05	2.163E-05	2.163E-05	2.163E-05
25	50	2.752E-05	2.920E-05	2.929E-05	2.929E-05	2.929E-05
x [m]	y [m]	N =10	N =20	N =40	N =80	N =160
25	32	-7.217E-07	4.318E-08	2.558E-08	2.563E-08	2.563E-08
25	34	-1.422E-06	1.470E-07	1.162E-07	1.161E-07	1.161E-07
25	40	4.741E-06	3.665E-06	3.661E-06	3.661E-06	3.661E-06
25	46	2.175E-05	2.155E-05	2.163E-05	2.163E-05	2.163E-05
25	50	2.713E-05	2.938E-05	2.929E-05	2.929E-05	2.929E-05

^{234}U

x [m]	y [m]	M =200	M =400	M =800	M =1,600	M =3,200
25	34	3.937E-05	4.038E-05	4.022E-05	4.019E-05	4.019E-05
25	36	2.029E-04	2.162E-04	2.160E-04	2.159E-04	2.159E-04
25	42	5.649E-03	7.897E-03	7.936E-03	7.936E-03	7.936E-03
25	46	2.695E-02	2.593E-02	2.565E-02	2.564E-02	2.564E-02
25	50	2.913E-02	3.552E-02	3.585E-02	3.586E-02	3.586E-02
x [m]	y [m]	N =10	N =20	N =40	N =80	N =160
25	34	-2.184E-03	1.134E-04	4.038E-05	4.019E-05	4.019E-05
25	36	-2.113E-03	1.975E-04	2.158E-04	2.159E-04	2.159E-04
25	42	1.118E-02	8.092E-03	7.936E-03	7.936E-03	7.936E-03

25	46	2.580E-02	2.544E-02	2.564E-02	2.564E-02	2.564E-02
25	50	3.262E-02	3.608E-02	3.586E-02	3.586E-02	3.586E-02

669

670 ^{230}Th

x [m]	y [m]	M =800	M =1,600	M =3,200	M =6,400	M =12,800
25	36	3.192E-08	3.181E-08	3.180E-08	3.179E-08	3.179E-08
25	38	1.578E-07	1.576E-07	1.576E-07	1.576E-07	1.576E-07
25	44	3.838E-06	3.914E-06	3.914E-06	3.914E-06	3.914E-06
25	48	8.531E-06	8.539E-06	8.539E-06	8.539E-06	8.539E-06
25	50	9.253E-06	9.261E-06	9.261E-06	9.262E-06	9.262E-06
x [m]	y [m]	N =10	N =20	N =40	N =80	N =160
25	36	-6.448E-07	2.862E-08	3.167E-08	3.179E-08	3.179E-08
25	38	-1.271E-07	1.141E-07	1.577E-07	1.576E-07	1.576E-07
25	44	4.705E-06	3.925E-06	3.914E-06	3.914E-06	3.914E-06
25	48	7.869E-06	8.534E-06	8.540E-06	8.539E-06	8.539E-06
25	50	8.345E-06	9.353E-06	9.261E-06	9.262E-06	9.262E-06

671 ^{226}Ra

x [m]	y [m]	M =100	M =200	M =400	M =800	M =1600
25	12	1.268E-08	1.273E-08	1.272E-08	1.272E-08	1.272E-08
25	18	4.817E-08	4.822E-08	4.821E-08	4.821E-08	4.821E-08
25	26	2.830E-07	2.824E-07	2.824E-07	2.824E-07	2.824E-07
25	42	8.794E-06	7.484E-06	7.578E-06	7.579E-06	7.579E-06
25	50	1.761E-05	1.449E-05	1.494E-05	1.497E-05	1.497E-05
x [m]	y [m]	N =10	N =20	N =40	N =80	N =160
25	12	8.791E-08	1.264E-08	1.272E-08	1.272E-08	1.272E-08
25	18	-1.512E-07	4.713E-08	4.821E-08	4.821E-08	4.821E-08
25	26	5.221E-07	2.830E-07	2.824E-07	2.824E-07	2.824E-07
25	42	7.960E-06	7.587E-06	7.578E-06	7.579E-06	7.579E-06
25	50	1.458E-05	1.498E-05	1.494E-05	1.497E-05	1.497E-05

672

673

674 **Table 8**

675 Transport parameters used for verification example 2 involving the ten-species transport problem
676 used by Srinivasan and Clement (2008b)

Parameter	Value
Domain length, L [m]	250
Domain width, W [m]	100
Seepage velocity, v [m year^{-1}]	5
Longitudinal Dispersion coefficient, D_L [m^2 year^{-1}]	50
Transverse Dispersion coefficient, D_T [m^2 year^{-1}]	50
Retardation coefficient, R_i	
i=1, 2,…,10	1.9, 1, 1.4, 1, 5, 8, 1.4, 3.1, 1, 1
Decay constant, k_i [year^{-1}]	
i=1, 2,…,10	3, 2, 1.5, 1.25, 2.75, 1, 0.75, 0.5, 0.25, 0.1
Source decay constant, λ_m [year^{-1}]	0.1, 0.75, 0.5, 0.25, 0, 0, 0.3, 1, 0, 0.65
m=1, 2,…,10	

677

678

679

680

Table 9

Coefficients of Bateman-type boundary source for ten-species transport problem used by Srinivasan and Clement (2008b)

Species, *i*	b_{im}									
	m=1	*m*=2	*m*=3	*m*=4	*m*=5	*m*=6	*m*=7	*m*=8	*m*=9	*m*=10
Species 1	10									
Species 2	0	5								
Species 3	0	0	2.5							
Species 4	0	0	0	0						
Species *5*	0	0	0	0	10					
Species *6*	0	0	0	0	0	5				
Species *7*	0	0	0	0	0	0	2.5			
Species *8*	0	0	0	0	0	0	0	0		
Species *9*	0	0	0	0	0	0	0	0	0	
Species *10*	0	0	0	0	0	0	0	0	0	0

688

689 **Table 10**

690 Transport parameters used for example application involving the five-species dissolved chlorinated
691 solvent problem used by BIOCHLOR.

Parameter	Value
Domain length, L [m]	330.7
Domain width, W [m]	213.4
Seepage velocity, v [m year^{-1}]	34.0
Longitudinal dispersion coefficient, D_L [m^2 year^{-1}]	449
Transverse dispersion coefficient, D_T [m^2 year^{-1}]	44.9
Retardation coefficient, R_i [-]	
PCE	7.13
TCE	2.87
DCE	2.8
VC	1.43
ETH	5.35
Decay constant, k_i [year^{-1}]	
PCE	2
TCE	1
DCE	0.7
VC	0.4
ETH	0
Source decay rate constant, λ_m [year^{-1}]	
PCE	0
TCE	0
DCE	0
VC	0
ETH	0

692 **Table 11**

693 Coefficients of Bateman-type boundary source used for example application involving the five-
694 species dissolved chlorinated solvent problem used by BIOCHLOR.

	b_{im}				
Species, *i*	*m=1*	*m=2*	*m=3*	*m=4*	*m=5*
PCE , i=1	0.056				
TCE , i=2		15.8			
DCE , i=3			98.5		
VC , i=4				3.08	
ETH , i=5					0.03

695

696

697

698

699

700

701

702

Figures Captions

Fig. 1. Schematic representation of two-dimensional transport of decaying contaminants in a uniform flow field with flux boundary source located at of the inlet boundary.

Fig. 2. Comparison of spatial concentration profiles of four species along the longitudinal direction (=50 m) at t = 1,000 years obtained from derived analytical solutions and numerical solutions for convergence test example 1 of four-member radionuclide decay chain $^{238}Pu \rightarrow ^{234}U \rightarrow ^{230}Th \rightarrow ^{226}Ra$.

Fig. 3. Comparison of spatial concentration profiles of four species along the transverse direction (=0 m) at t = 1,000 years obtained from derived analytical solutions and numerical solutions for convergence test example 1 of four-member radionuclide decay chain $^{238}Pu \rightarrow ^{234}U \rightarrow ^{230}Th \rightarrow ^{226}Ra$.

Fig. 4. Comparison of spatial concentration profiles of four species along the transverse direction (=25 m) at t = 1,000 years obtained from derived analytical solutions and numerical solutions for convergence test example 1 of four-member radionuclide decay chain $^{238}Pu \rightarrow ^{234}U \rightarrow ^{230}Th \rightarrow ^{226}Ra$.

Fig. 5. Comparison of spatial concentration profiles of four species along the longitudinal direction (=50 m) at t = 1,000 years obtained from derived analytical solutions and numerical solutions for convergence test example 2 of four-member radionuclide decay chain $^{238}Pu \rightarrow ^{234}U \rightarrow ^{230}Th \rightarrow ^{226}Ra$.

Fig. 6. Comparison of spatial concentration profiles of four species along the transverse direction (=0 m) at t = 1,000 years obtained from derived analytical solutions and numerical solutions for convergence test example 2 of four-member radionuclide decay chain

725 $^{238}Pu \rightarrow ^{234}U \rightarrow ^{230}Th \rightarrow ^{226}Ra$.

726 Fig. 7. Comparison of spatial concentration profiles of four species along the transverse direction
727 (=25 m) at t = 1,000 years obtained from derived analytical solutions and numerical
728 solutions for convergence test example 2 of four-member radionuclide decay chain
729 $^{238}Pu \rightarrow ^{234}U \rightarrow ^{230}Th \rightarrow ^{226}Ra$.

730 Fig. 8. Comparison of spatial concentration profiles of ten-species along x-direction at t = 20 days
731 obtained from derived analytical solutions and numerical solutions for the test example 3
732 of ten species decay chain used by Srinivasan and Clement (2008b).

733 Fig. 9. Effects of physical processes and chemical reactions on the concentration contours of four-
734 species at t = 1,000 years obtained from derived analytical solutions for four-member decay
735 chain $^{238}Pu \rightarrow ^{234}U \rightarrow ^{230}Th \rightarrow ^{226}Ra$.

736 Fig. 10. Spatial concentration contours of five-species at t = 1 year obtained from derived analytical
737 solutions for natural attenuation of chlorinated solvent plumes $PCE \rightarrow TCE \rightarrow DCE \rightarrow VC$
738 $\rightarrow ETH$.

739

740

741

742

743

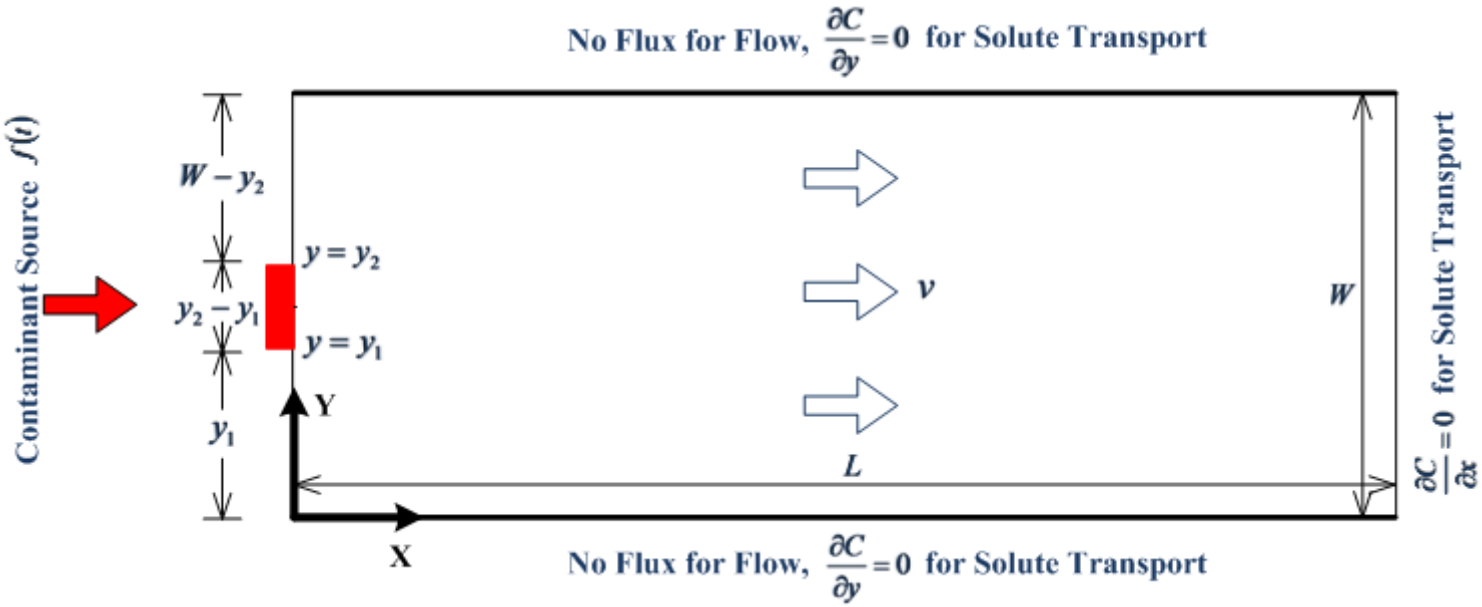
No Flux for Flow, $\frac{\partial C}{\partial y}=0$ for Solute Transport
Contaminant Source $f(t)$
$W-y_2$
$y=y_2$
y_2-y_1
$y=y_1$
y_1
Y
X
v
L
W
$\frac{\partial C}{\partial x}=0$ for Solute Transport
No Flux for Flow, $\frac{\partial C}{\partial y}=0$ for Solute Transport

Fig. 1.

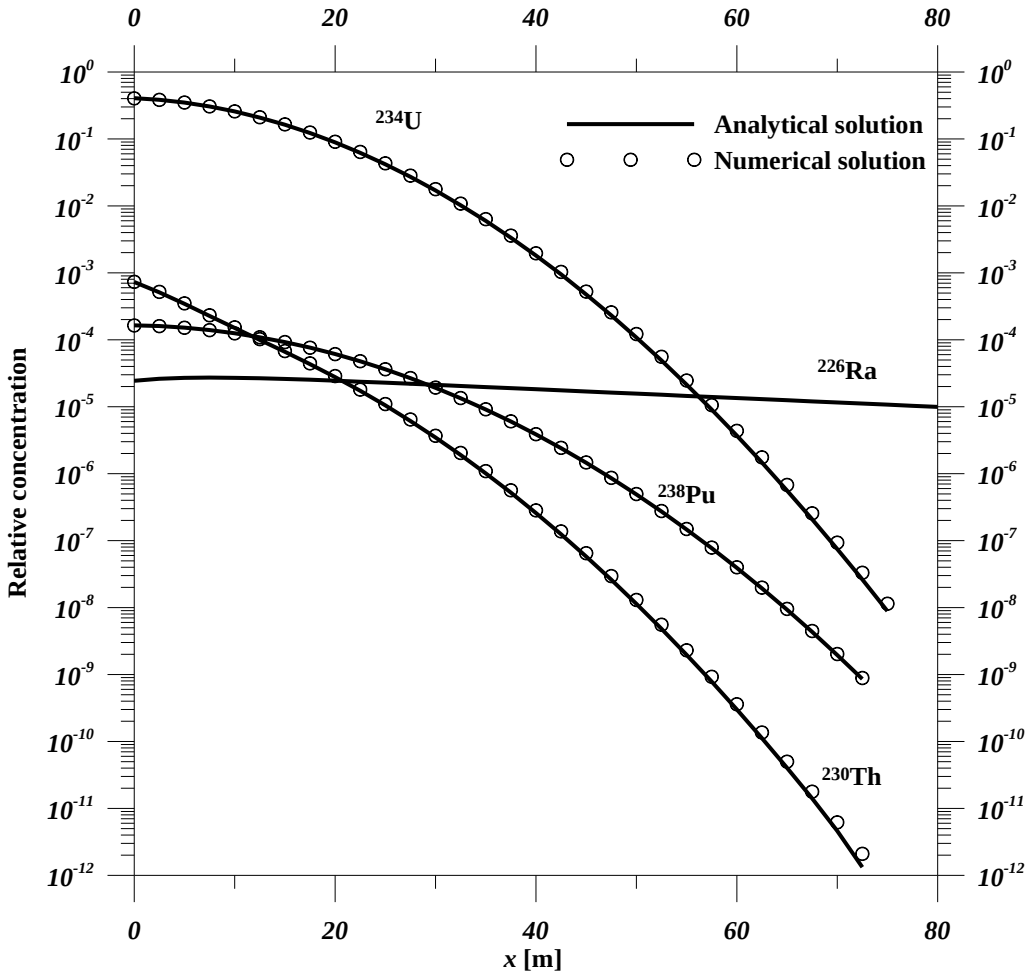
0
20
40
60
80
10^{0}
10^{-1}
10^{-2}
10^{-3}
10^{-4}
10^{-5}
10^{-6}
10^{-7}
10^{-8}
10^{-9}
10^{-10}
10^{-11}
10^{-12}
Relative concentration
^{234}U
^{226}Ra
^{238}Pu
^{230}Th
Analytical solution
Numerical solution
x [m]

Fig. 2.

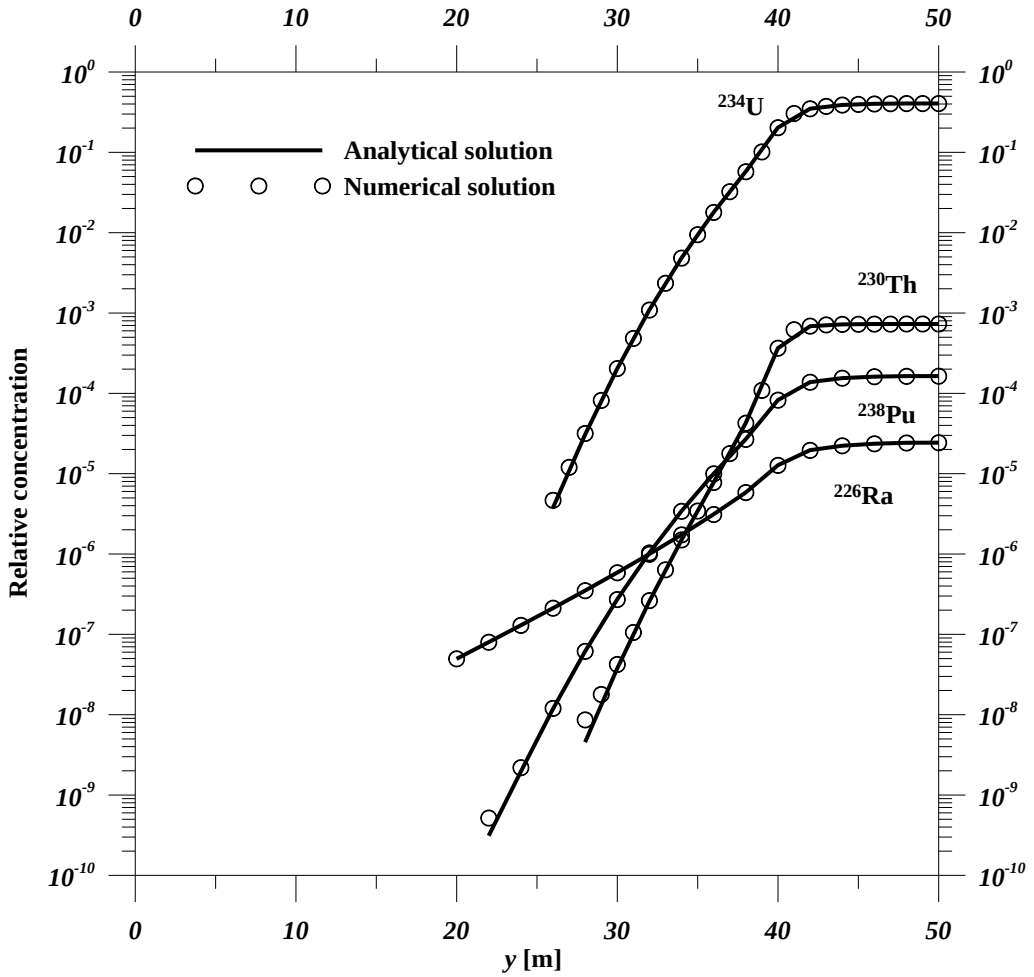
Analytical solution
Numerical solution
234U
230Th
238Pu
226Ra
Relative concentration
y [m]
0
10
20
30
40
50
10^0
10^-1
10^-2
10^-3
10^-4
10^-5
10^-6
10^-7
10^-8
10^-9
10^-10

Fig. 3

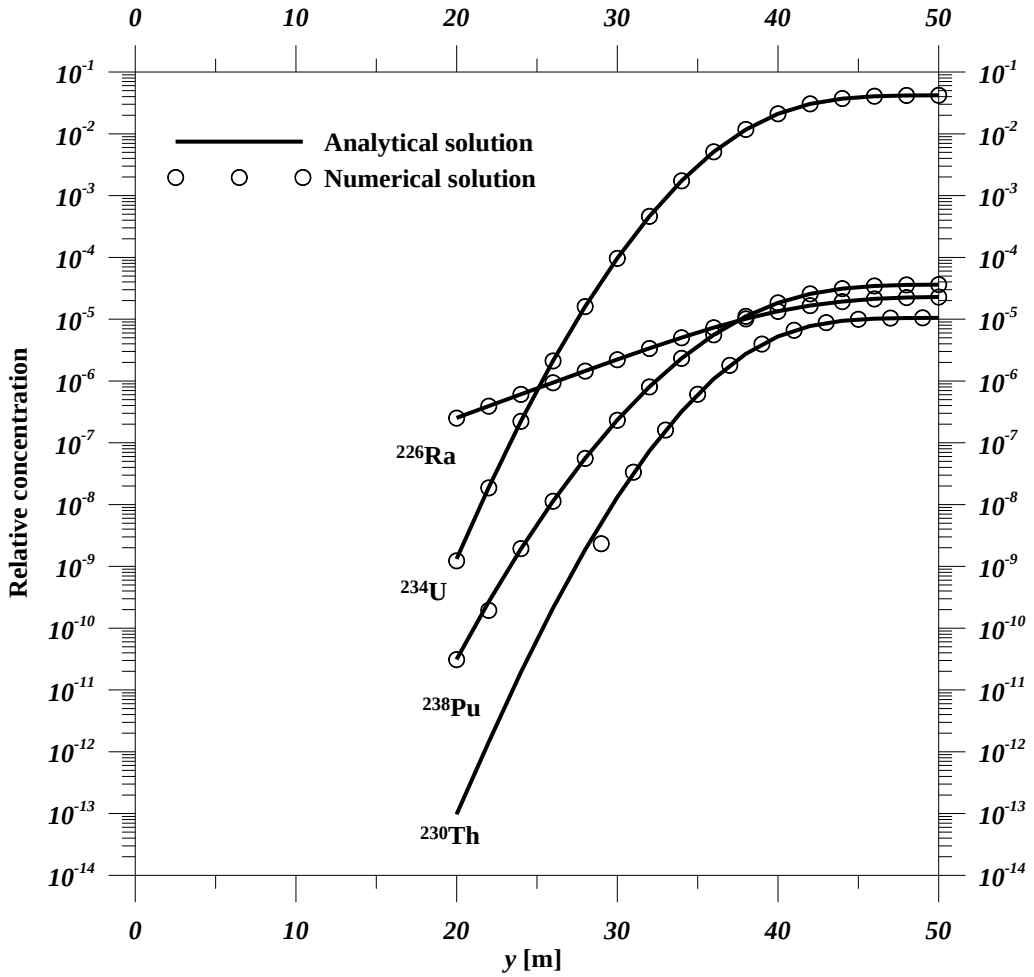
Analytical solution
Numerical solution
226Ra
234U
238Pu
230Th
Relative concentration
y [m]
0
10
20
30
40
50
10-1
10-2
10-3
10-4
10-5
10-6
10-7
10-8
10-9
10-10
10-11
10-12
10-13
10-14

Fig. 4

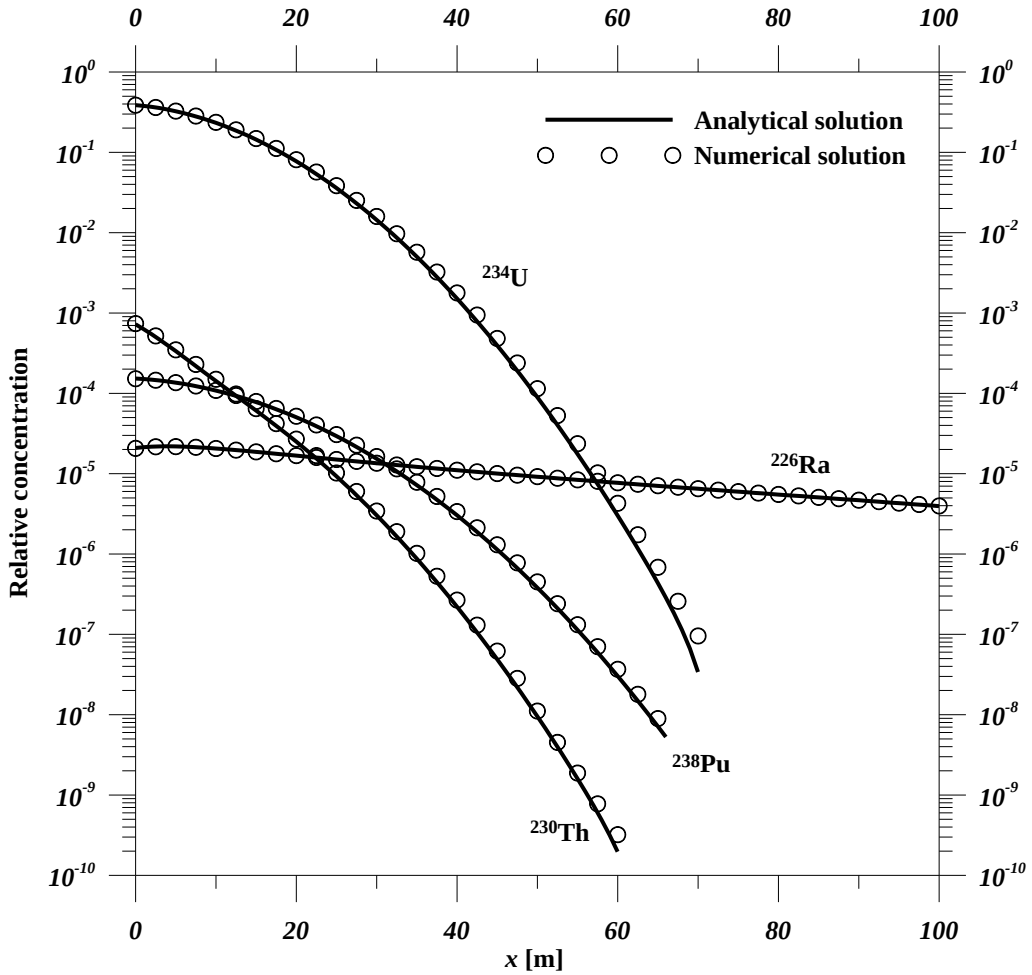
Analytical solution
Numerical solution
234U
226Ra
238Pu
230Th
Relative concentration
x [m]
0
20
40
60
80
100
10^0
10^-1
10^-2
10^-3
10^-4
10^-5
10^-6
10^-7
10^-8
10^-9
10^-10

Fig. 5

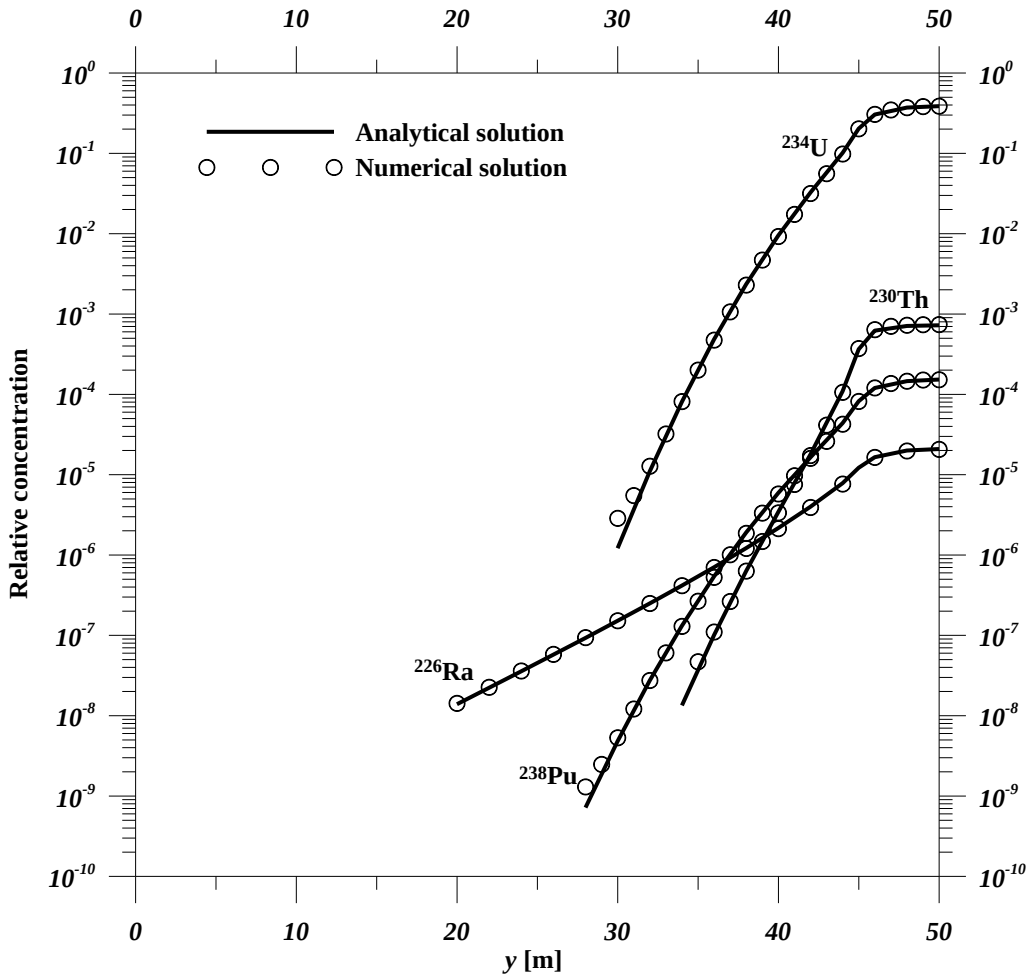
Analytical solution
Numerical solution
234U
230Th
226Ra
238Pu
Relative concentration
y [m]
0
10
20
30
40
50
10^0
10^-1
10^-2
10^-3
10^-4
10^-5
10^-6
10^-7
10^-8
10^-9
10^-10

Fig. 6

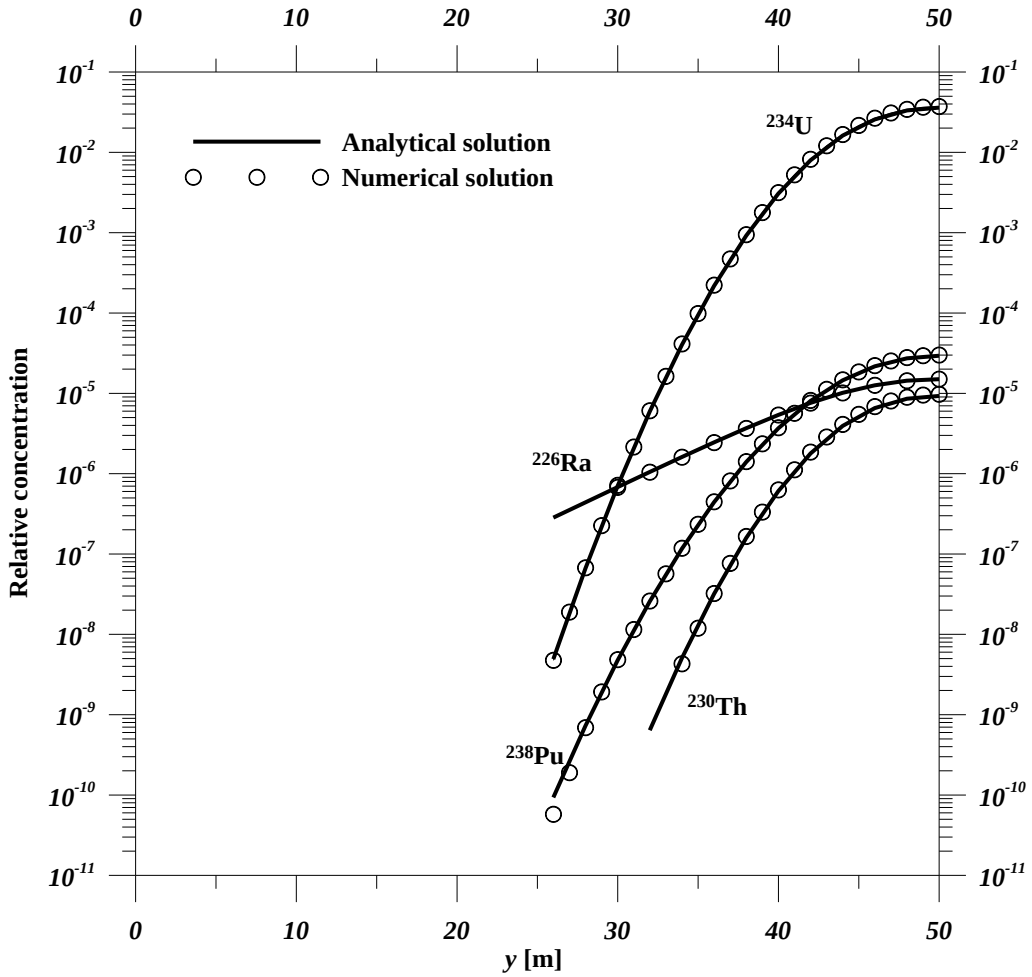
Analytical solution
Numerical solution
234U
226Ra
230Th
238Pu
Relative concentration
y [m]
0
10
20
30
40
50
10-1
10-2
10-3
10-4
10-5
10-6
10-7
10-8
10-9
10-10
10-11

Fig. 7

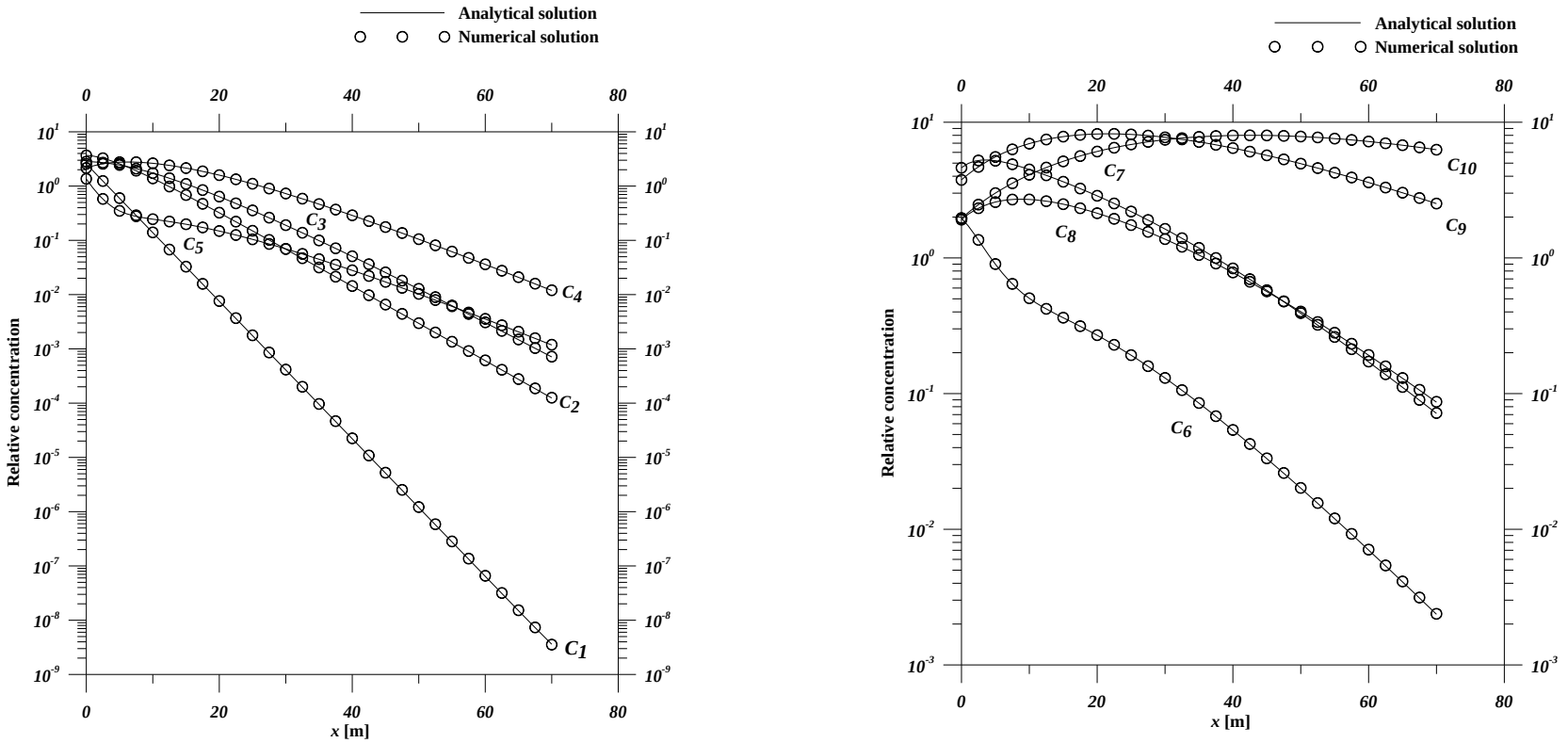
Analytical solution
Numerical solution
Relative concentration
x [m]
C1
C2
C3
C4
C5
C6
C7
C8
C9
C10

Fig. 8

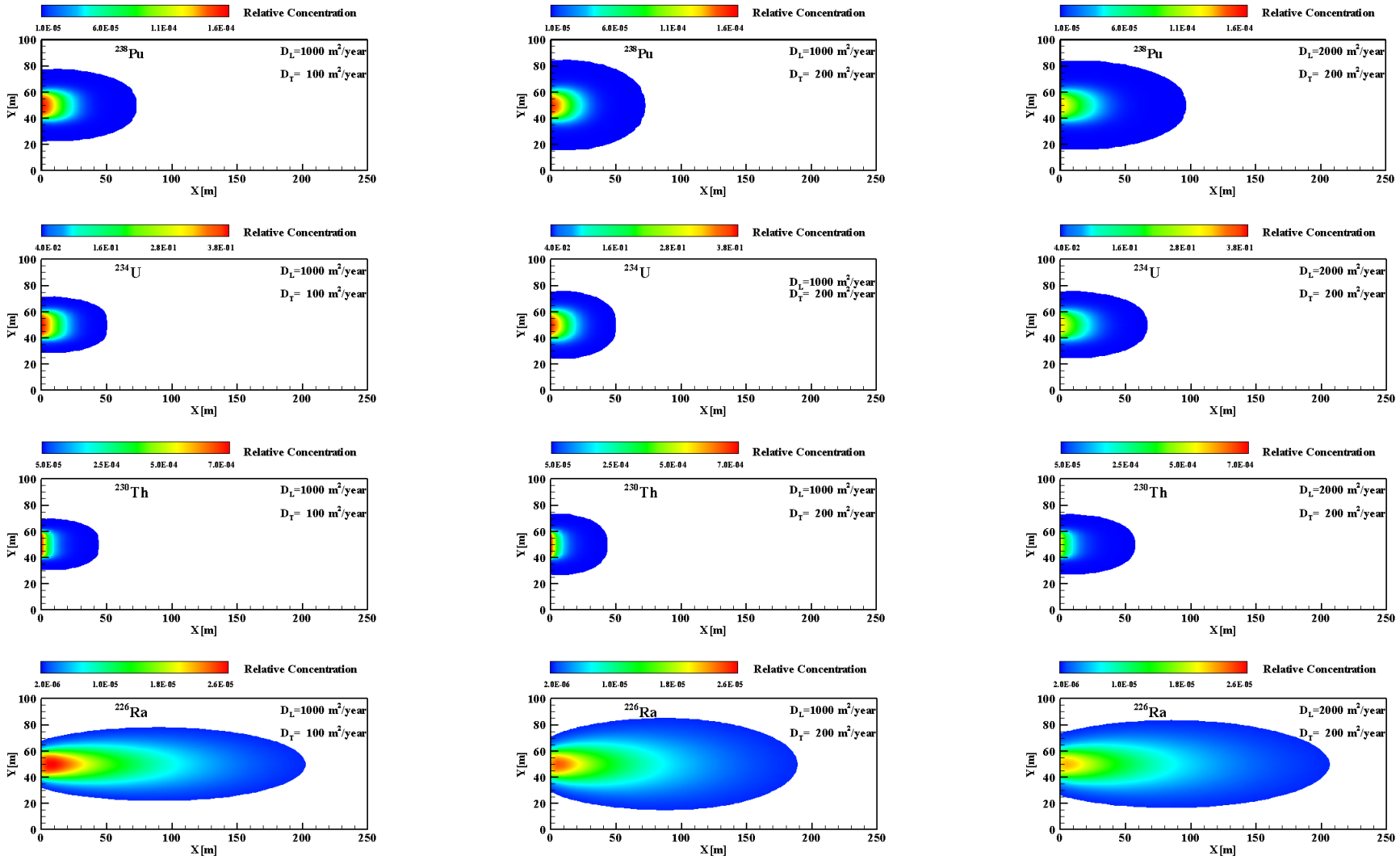
Relative Concentration
1.0E-05 6.0E-05 1.1E-04 1.6E-04
238Pu
DL=1000 m2/year
DT= 100 m2/year
DT= 200 m2/year
DL=2000 m2/year
DT= 200 m2/year
4.0E-02 1.6E-01 2.8E-01 3.8E-01
234U
5.0E-05 2.5E-04 5.0E-04 7.0E-04
230Th
2.0E-06 1.0E-05 1.8E-05 2.6E-05
226Ra
X [m]
Y [m]

Fig. 9

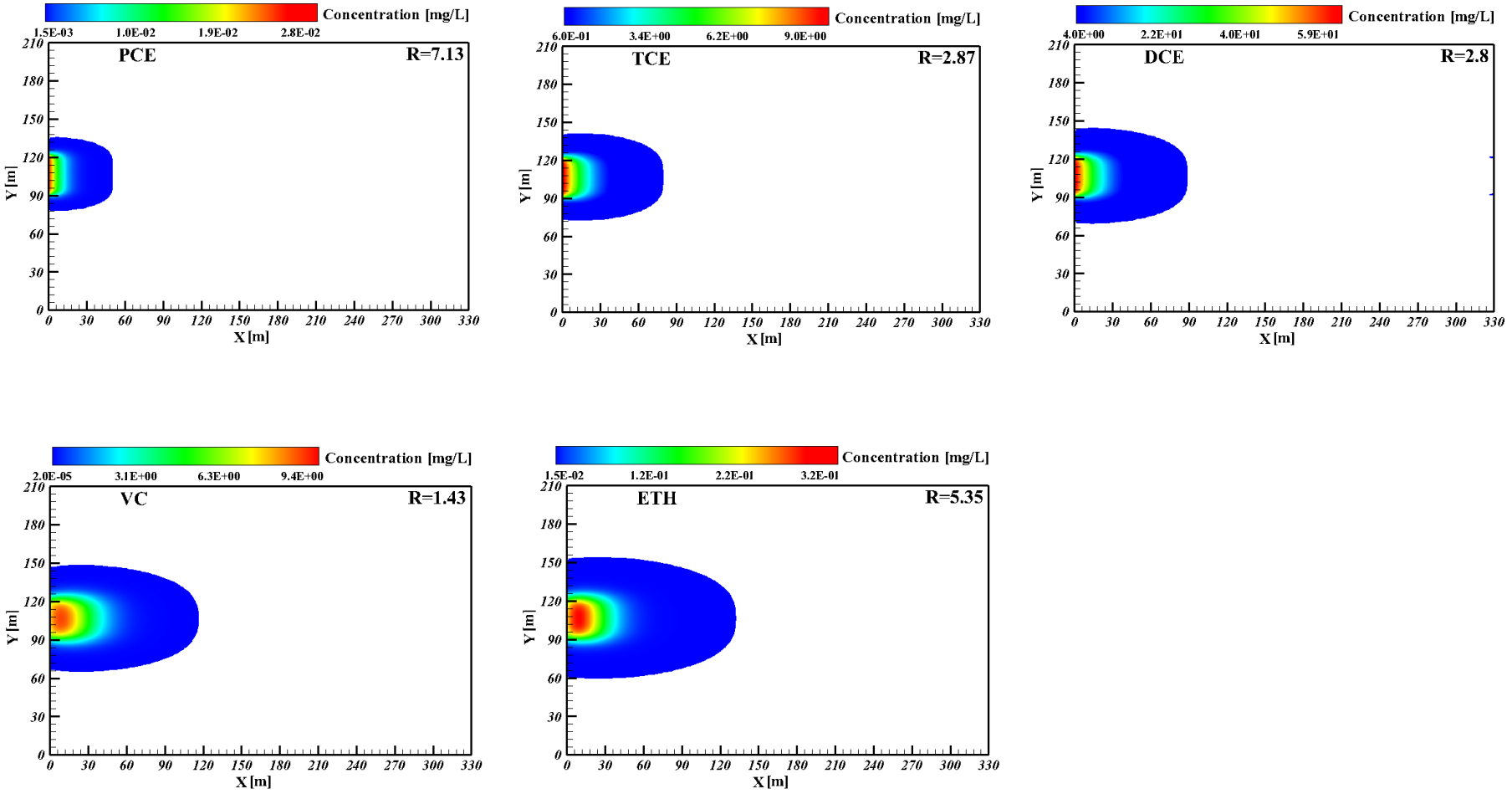
Concentration [mg/L]
1.5E-03
1.0E-02
1.9E-02
2.8E-02
PCE
R=7.13
Concentration [mg/L]
6.0E-01
3.4E+00
6.2E+00
9.0E+00
TCE
R=2.87
Concentration [mg/L]
4.0E+00
2.2E+01
4.0E+01
5.9E+01
DCE
R=2.8
Concentration [mg/L]
2.0E-05
3.1E+00
6.3E+00
9.4E+00
VC
R=1.43
Concentration [mg/L]
1.5E-02
1.2E-01
2.2E-01
3.2E-01
ETH
R=5.35
Y [m]
X [m]
0
30
60
90
120
150
180
210
240
270
300
330

Fig. 10